

Review

Oscillating-water-column wave energy converters and air turbines: A review



António F.O. Falcão*, João C.C. Henriques

IDMEC, LAETA, Instituto Superior Técnico, Universidade de Lisboa, 1049-001, Lisbon, Portugal

ARTICLE INFO

Article history:

Received 9 March 2015

Received in revised form

18 July 2015

Accepted 29 July 2015

Available online 25 August 2015

Keywords:

Wave energy

Oscillating water column

Air turbines

Modelling

Control

Review

ABSTRACT

The ocean waves are an important renewable energy resource that, if extensively exploited, may contribute significantly to the electrical energy supply of countries with coasts facing the sea. A wide variety of technologies has been proposed, studied, and in some cases tested at full size in real ocean conditions. Oscillating-water-column (OWC) devices, of fixed structure or floating, are an important class of wave energy devices. A large part of wave energy converter prototypes deployed so far into the sea are of OWC type. In an OWC, there is a fixed or floating hollow structure, open to the sea below the water surface, that traps air above the inner free-surface. Wave action alternately compresses and decompresses the trapped air which is forced to flow through a turbine coupled to a generator. The paper presents a comprehensive review of OWC technologies and air turbines. This is followed by a survey of theoretical, numerical and experimental modelling techniques of OWC converters. Reactive phase control and phase control by latching are important issues that are addressed, together with turbine rotational speed control.

© 2015 Elsevier Ltd. All rights reserved.

1. Introduction

The ocean waves are an important renewable energy resource that, if extensively exploited, may contribute significantly to the electrical energy supply of countries with coasts facing the ocean [1]. A wide variety of technologies has been proposed, studied, and in some cases tested at full size in real ocean conditions [2–5]. The mechanical process of energy absorption from the waves requires a moving interface, involving (i) a partly or totally submerged moving body and/or (ii) a moving air–water interface subject to a time-varying pressure. In the latter case, there is a fixed or oscillating hollow structure, open to the sea below the water surface, that traps air above the inner free-surface; wave action alternately compresses and decompresses the trapped air which forces air to flow through a turbine coupled to a generator. Such a device is named oscillating-water-column (OWC). Although the concept was already known in the 1940s, this designation seems to have appeared for the first time in published paper form in 1978 [6] and has been widely used ever since, even if the moving water inside the structure is far from shaped like a column. Before that, this type

of wave energy converter (WEC) was sometimes known as the Masuda device. The main advantage of the OWC versus most other WECs is its simplicity: the only moving part of the energy conversion mechanism is the rotor of a turbine, located above water level, rotating at a relatively high velocity and directly driving a conventional electrical generator. OWCs are a major class of wave energy converters, possibly the class that has been most extensively studied and with the largest number of prototypes so far deployed into the sea.

In almost all OWCs, the air alternately flows from the chamber to the atmosphere and back, although in some concepts the flow is in closed circuit. Unless rectifying valves are used, which is widely regarded as unpractical except possibly in small devices like navigation buoys, the turbines are self-rectifying, i.e. their rotational direction remains unchanged regardless of the direction of the air flow. Several types of such special turbines have been developed. The axial-flow Wells turbine, invented in the mid-1970s, is the most popular self-rectifying turbine, but other types, namely self-rectifying impulse turbines, have also been proposed, studied and used.

Apart from reviews on WECs in general [2–5], more specific reviews on OWCs can be found in Refs. [7,8]. Reviews on air turbines for OWCs were published in Refs. [9–13]. A detailed historical description, until about 1995, of the development of wave energy

* Corresponding author.

E-mail address: antonio.falcao@ist.utl.pt (A.F.O. Falcão).

Nomenclature

Roman letters

A	added mass
B	radiation force coefficient
c	blade chord (Section 3)
D	turbine rotor diameter
E	energy per unit mass (Section 3)
f_e, f_r	excitation force, radiation force
F_e, F_r	complex amplitudes of f_e, f_r
g	acceleration of gravity
G	radiation conductance
H	radiation susceptance
k	polytropic exponent
m	mass
p	pressure
P	complex amplitude of p
P_t	turbine power
q	volume flow rate
Q	complex amplitude of q
S	inner free-surface area
t	cascade pitch (Section 3)

t time

T torque

U blade velocity

V absolute flow velocity (Section 3)

V air chamber volume (Section 4)

w mass flow rate

x vertical coordinate

X complex amplitude of x

Greek letters

α	absolute flow velocity angle
β	relative flow velocity angle
η	turbine efficiency
Π	dimensionless turbine power
ρ	density
σ	standard deviation (or rms)
ϕ	flow rate coefficient (Section 3)
Φ	dimensionless flow rate
ψ	pressure coefficient (Section 3)
Ψ	dimensionless pressure head
ω	radian frequency
Ω	rotational speed

conversion in general, and OWCs in particular, can be found in Ref. [14], a book written from a non-technical point of view by a freelance journalist.

The present review paper concentrates on what is specific of OWC wave energy converters. Issues like moorings, electrical equipment and environmental impact (except air turbine noise) that are common to other wave energy technologies are left out. A review of OWC technologies is presented in Section 2. This is followed, in Section 3, by a review of air turbines for OWC applications, especially self-rectifying turbines. Section 4 is devoted to theoretical, numerical and experimental modelling techniques of OWC converters. Phase control and rotational speed control are dealt with in Section 5. Conclusions are presented in Section 6.

2. OWC technology

2.1. Early developments until 1990

Yoshio Masuda (1925–2009) (Fig. 1), a Japanese navy officer, may be regarded as the father of modern wave energy technology, with studies in Japan since the second half of the 1940s. He developed a navigation buoy powered by wave energy, equipped with an air turbine (Fig. 2), which was in fact what was later named as a (floating) OWC [15–17]. Such buoys were commercialized in large numbers in Japan since 1965 (and later in USA), and were the first wave energy devices successfully deployed into the sea. Masuda's navigation buoys were equipped with a conventional unidirectional air turbine, which required a system of rectifying valves (Fig. 2).

The first large-scale WEC to be deployed into the sea was the Kaimei, another creation of Yoshio Masuda, built for the Japan Marine Science and Technology Centre (JAMSTEC). Kaimei was a large barge (80 m × 12 m, 820 ton) that had thirteen OWC open-bottom chambers built into the hull, each having a water plane area of 42–50 m² (Fig. 3). It was deployed off the western coast of Japan in 1978–80 and again in 1985–86 [17,18]. Eight unidirectional air turbines were tested in 1978–80 with various non-return

rectifying valve arrangements; in 1985–86, three unidirectional turbines were tested together with two self-rectifying turbines.

In Europe, studies to develop large scale WECs were initiated about 1973, shortly after the oil crisis. An ambitious government program started in UK in 1975, the aim being a large, 2 GW wave energy plant [14,19]. The development of several types of WECs was funded, including OWCs. The National Engineering Laboratory (NEL), in Scotland, studied different concepts for a large OWC plant. This converged into a design consisting of a set of bottom-standing structures, shaped as a breakwater, each housing a series of OWCs, Fig. 4 (by then, the self-rectifying Wells turbine had already been invented). The British wave energy program was abruptly terminated in 1982, without any full-sized prototype having been constructed.

The less ambitious Norwegian program went on to install in 1985 a full-sized OWC integrated into a cliff at Toftestallen, near Bergen (Fig. 5). The plant was equipped with a vertical-axis Wells turbine, and was nominally rated at 500 kW. Nothing was published about the plant performance, but it was unofficially known that it was rather lower than expected. The plant was destroyed in 1988 during a storm due to failure of the bolted connection of the steel structure to the concrete foundation. In the following years, until the early 1990s, the activity in Europe remained mainly at the academic level, the most visible achievement being a small (75 kW) OWC shoreline prototype, equipped with a Wells turbine, deployed at the island of Islay, Scotland (commissioned in 1991), Fig. 6 [20].

Before that, a shore-fixed OWC (chamber area about 45 m²) equipped with a 40 kW Wells turbine (previously tested in Kaimei) was installed in 1983 in the Sea of Japan, at Sanze 1990 [17]. This was followed, in Asia, by the installation, about 1990, of two larger OWC prototypes: a 60 kW converter integrated into a breakwater at the port of Sakata, Japan, (Fig. 7) [21,22] and a bottom-standing 125 kW plant at Trivandrum, India, (Fig. 8) [23]. Both were equipped with Wells turbines. Later, the Indian plant was used to test different types of air turbines, including impulse turbines [24]. The Sakata OWC was the first (and for many years only) case of integration of a wave energy converter into a breakwater, as a way of sharing the costs of the structure. This conception was recently



Fig. 1. Yoshio Masuda in 2001.

adopted in Spain and Italy (see Section 2.2.2).

The Kaimei tests revealed that, although the efficiency of the air turbines was not far from what was expected, the hydrodynamic performance of wave energy absorption was quite disappointing.

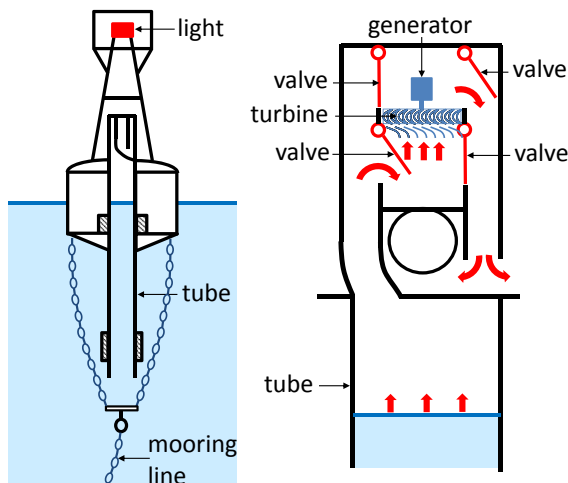


Fig. 2. Layout of Masuda's navigation buoy (based on [10]). On the right-hand-side, details of the air flow through the turbine and rectifying valves.

Yoshio Masuda and his team then devised other concepts for floating OWCs. The main outcome of this exercise was the Backward Bent Duct Buoy (BBDB) [17]. The BBDB is a floating device with an L-shaped OWC, a buoyancy caisson-type module, an air chamber and an air turbine driving an electrical generator (Fig. 9). Since there is no vertical central tube, the converter does not need deep water for deployment. Devices with the submerged duct opening facing the incident waves were first studied, with no plans to test a backward facing duct. Then, quite surprisingly, it was found that a better performance could be achieved by positioning the device with its back facing the waves, as shown in Fig. 9. Laboratory tests, with a model 2.41 m long, were first performed in Japan about 1986 [17].

2.2. Developments since the early 1990s

2.2.1. Fixed-structure OWCs

The situation in Europe was dramatically changed by the decision made in 1991 by the European Commission of including wave energy in their R&D program on renewable energies. This lead to the basic studies, followed by the design and construction, of two full-sized fixed-structure OWC plants (the so-called European pilot plants), one on the island of Pico, Azores, Portugal, and the other on the island of Islay, Scotland, UK. Both were equipped with Wells turbines. The Pico plant, rated 400 kW, was completed in 1999 and is still operational. It was built, standing on the sea bottom, adjacent to a vertical cliff (Fig. 10) [25]. The Islay plant, completed in 2000 and rated 500 kW, was built in a recess carved into a rocky cliff (Fig. 11) [26]. Another shoreline OWC plant, rated 100 kW, was built in 2001 in Guangdong Province, China (Fig. 12) [27]. A few years earlier, a large nearshore bottom-standing OWC (named OSPREY), rated 1 MW, was destroyed by the sea shortly after having been towed and sunk into place near the Scottish coast in 1995. A large bottom-standing OWC, the greenWAVE, rated 1 MW, was recently constructed by the Australian company Oceanlinx (Fig. 13). An accident to the airbags supporting the 3000-tonne structure occurred in March 2014 when the plant was being towed from Port Adelaide to Port MacDonnell, in western Australia, forcing the plant to be left aground.

A recently completed bottom-standing OWC, rated 500 kW, was installed at Yongsoo, about 1 km off the coast of Jeju Island, South Korea (Fig. 14). The plant is 37 m long and 31.2 m wide.

It has been found since the early 1980s that the wave energy absorption process can be enhanced by extending the chamber structure by protruding (natural or man-made) walls in the direction of the waves, forming a harbour or a collector [28,29]. This concept was put into practice in some of the early OWC prototypes,



Fig. 3. The Kaimei.

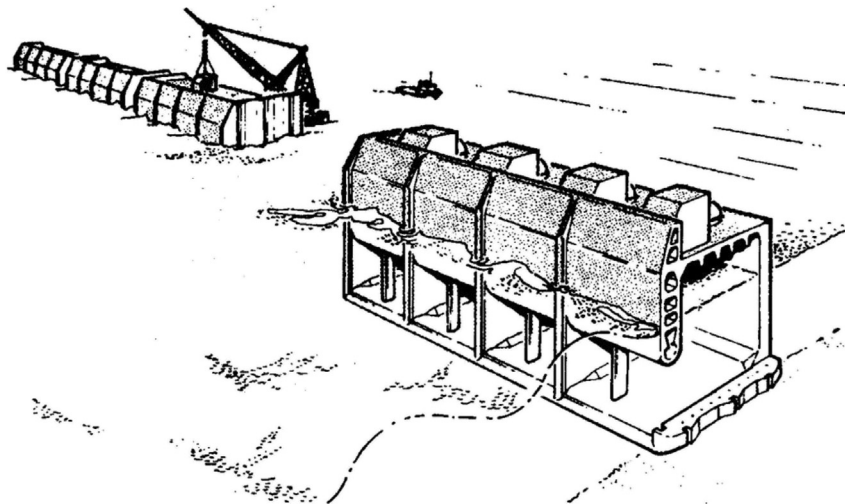


Fig. 4. The design of the NEL breakwater OWC.

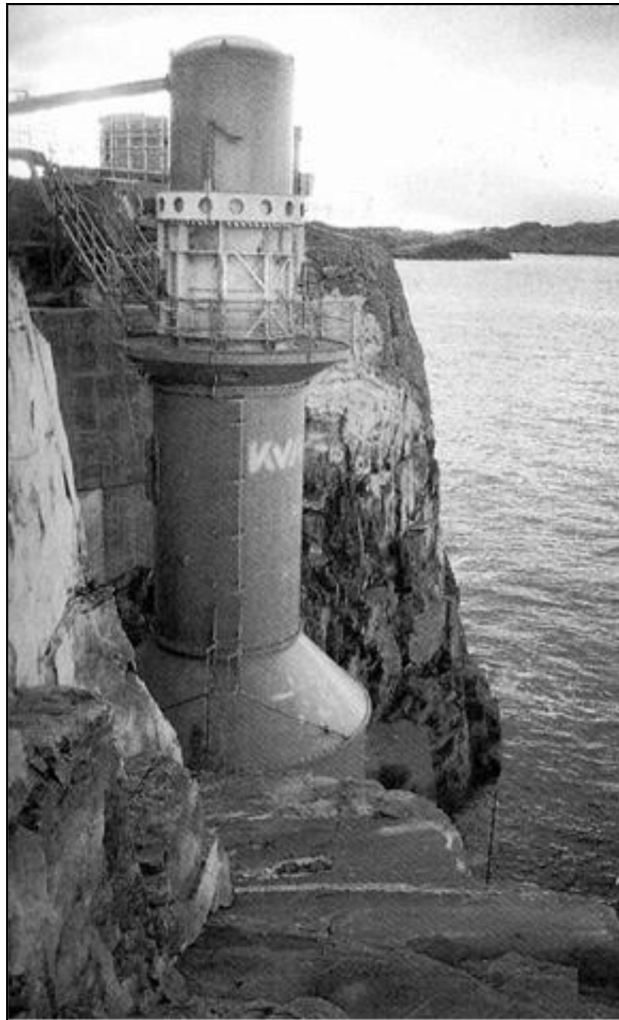


Fig. 5. Shoreline OWC at Toftestallen, near Bergen, Norway, about 1985.

namely in Toftestallen, Norway (Fig. 5) and Trivandrum, India (Fig. 8). The Australian company Energetech developed a technology using a parabolic-shaped collector for this purpose. A bottom-

standing nearshore prototype, whose structure was made of steel, was tested at Port Kembla, Australia, in 2005 [30] (Fig. 15).

2.2.2. Breakwater-integrated OWCs

The design and construction of the structure are the most critical issues in fixed-structure OWC technology, and the most influential on the economics of energy produced from the waves. The integration of the plant structure into a breakwater for coastal or harbour protection has several advantages: the construction costs are shared, and the access for construction, operation and maintenance of the wave energy plant becomes much easier. This has been done successfully for the first time in the harbour of Sakata, Japan, in 1990 (Fig. 7) [21], where one of the caissons making up the breakwater had a special shape to accommodate the OWC and the mechanical and electrical equipment. The option of the "breakwater OWC" was adopted in the breakwater constructed at the port of Mutriku, in northern Spain (2008–10) [31], with 16 chambers and 16 Wells turbines rated 18.5 kW each (Fig. 16).

A different geometry for an OWC embedded into a breakwater was proposed by Boccotti [32], with an OWC that is long in the wave crest direction but narrow (small aperture) in the fore-aft direction. The OWC cross-section is U-shaped, with its outer opening facing upwards (Fig. 17). An advantage of this conception is that it allows the total length of the water column to be increased without placing the opening too far below the sea surface. This type of OWC-breakwater is being constructed at the harbour of Civitavecchia (near Rome), Italy (Fig. 17), with 17 caissons and 136 OWCs, and is planned to be adopted for new breakwaters in Italy [33–35].

2.2.3. Floating-structure OWCs

Since the early model tests in Japan in the mid-1980s, the BBDB concept has been object of considerable interest in several countries (Europe, Japan, South Korea, USA, China, India), with theoretical/numerical and experimental studies [36–40]. A 1:4th-scale BBDB OWC (the OE Buoy) was tested in Galway Bay, Ireland, between 2008 and 2011 (Fig. 18) [41]. It was equipped first with a Wells turbine and later with an axial-flow self-rectifying impulse turbine [41,42].

The Mighty Whale, another floating OWC converter, was developed by the Japan Marine Science and Technology Center. The device consisted of a floating structure (length 50 m, breadth 30 m,



Fig. 6. Shoreline OWC on the island of Islay, Scotland, rated 75 kW, commissioned in 1991 (courtesy of M. Folley).



Fig. 7. OWC plant integrated into a breakwater at Sakata harbour, Japan, 1990. Rated power 60 kW.

draught 12 m, displacement 4400 ton) which had three air chambers located at the front, side by side, and buoyancy tanks (Fig. 19). Each air chamber was connected to a Wells air turbine. The total rated power was 110 kW. The device was deployed near the mouth of Gokasho Bay, in Mie Prefecture, Japan, in 1998 and tested for several years [43,44].

The Australian company Oceanlinx deployed, from February to May 2010, off Port Kembla, Australia, a one-third-scale grid-connected model of the 2.5 MW full-scale OWC device, the Mk3, which (like the Kaimei three decades earlier) is a floating platform with several OWC chambers (in this case eight chambers) each with an

air turbine. During the tests, only two turbines (of different types) were installed (Fig. 20).

The concept of an axisymmetric floating OWC, consisting of a relatively long vertical tube, open at both ends, attached to a floater, has been considered since the early pioneers of wave energy conversion. The length of the tube determines the resonance frequency of the inner water column. This device, sometimes named OWC spar-buoy, was object of two of the earliest journal papers devoted to the theoretical modelling of wave energy converters [45,46] and is analysed by McCormick in his pioneer book [47]. Several types of wave-powered navigation buoys have been based on this concept



Fig. 8. Bottom-standing OWC installed in 1990 at Trivandrum, southern India. Rated power 125 kW.

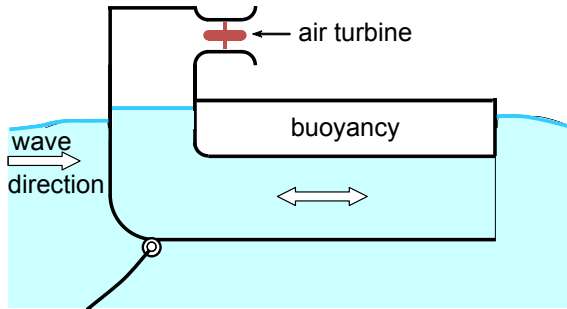


Fig. 9. Schematic representation of the Backward Bent Duct Buoy (BBDB).

[16,48], which has also been considered for larger scale energy production [49]. A report prepared for the British Department of Trade and Industry in 2005 [50] compared several types of floating OWCs for electricity generation in an Atlantic environment and considered the OWC spar-buoy to be the lowest risk and most economic option for further development. The OWC spar-buoy was object of optimization studies that showed the advantage of the tube being tapered at its lower part rather than cylindrical (Fig. 21) (see Refs. [51,52]).

2.2.4. Floating structure WECs with interior OWC

Some WEC configurations have been proposed and studied in which the OWC is enclosed in the floating structure and is not connected to the outer sea water.

The U-Gen device consists of an asymmetric floater with an interior U-tank partially filled with water and two lateral air chambers connected by a duct. The motion of the U-shaped OWC, mainly induced by the pitching of the floater, forces the air through the duct where a self-rectifying air turbine is installed to absorb the energy (Fig. 22). A 1:16th-scale model, 1.25 m long, was tested in 2010 at the IFREMER wave tank, in Brest, France [53]. Results from theoretical modelling are reported in Ref. [54]. A somewhat similar

device, using a water turbine of cross-flow type instead of an air turbine, was studied in Ref. [55]. Another pitching device with what can be considered as an interior OWC is described and theoretically modelled in Ref. [56]. It consists of a buoyant tethered submerged circular cylinder which is allowed to pitch freely about an axis below its centre. Within the body of the cylinder a fluid half fills an annular tank. The pitching motion of the cylinder in waves induces a sloshing motion inside the tank which in turns drives an air turbine connecting air chambers above the two isolated internal free surfaces.

An axisymmetric WEC recently proposed and analysed in Ref. [57] consists in an air-filled box that is fixed to the sea bottom or is floating (Fig. 23). The moving interface between the enclosed air and the surrounding sea water may be a rigid surface mounted on flexible bellows, or a rigid surface connected to the box walls in the manner of a loudspeaker diaphragm, or it may be made completely out of a flexible membrane. The box enclosed air space V_1 is connected to the atmosphere by an OWC whose walls are co-axial tubes, an air volume V_2 and an air turbine (Fig. 23). The OWC and the air compressibility play essential roles in the device dynamics. The required air volume is larger for the bottom-fixed device whose frequency response width was found to be substantially wider than that the floating version.

2.2.5. Multi-OWC devices

Apart from OWCs integrated into breakwaters, other WECs have been studied consisting of multiple OWCs. In some cases, several air chambers share a single unidirectional conventional air turbine, which requires low pressure and high pressure air ducts and rectifying air valves.

The Seabreath, under development at Padova University, Italy [58], is a floating attenuator, i.e. its elongated structure is aligned with the propagation direction of the incident waves (Fig. 24). It comprises a set of rectangular chambers with open bottom. Each OWC air chamber is connected by non-return valves to two longitudinal ducts (high pressure and low pressure) that feed a conventional unidirectional air turbine.



Fig. 10. Back view of the 400 kW OWC plant on the island of Pico, Azores, Portugal, 1999.



Fig. 11. LIMPET OWC plant, rated 500 kW, installed in 2000 on the island of Islay, Scotland, UK.

The LEANCON is another multi-OWC device. The OWCs are arranged in two rows under two beams connected to each other in a V-shaped fashion (Fig. 25). As in Seabreath, each OWC chamber is connected by non-return valves to two ducts that feed a conventional unidirectional air turbine. Model tests were performed in the deep wave tank of Aalborg University, in Denmark, using a 1:40th-scale model with a total of 120 OWC chambers or pipes [59].

A largely similar, although substantially smaller, device was numerically simulated and model tested at scale 1:50 at the large oceanic basin of the Hydraulics and Maritime Research Centre, located at University College Cork, Ireland [60]. The 32 OWC chambers are arranged along the two legs of a 90-degree V-shaped floating structure. Cross trusses between the two legs of the platform provide the necessary structural strength to enable the platform to survive sea conditions.

The capacity of OWCs to absorb wave energy prompted researchers [61–63] to propose the use of OWCs in reducing the

hydroelastic responses of very large floating structures (VLFS). For a review see Ref. [64].

2.3. Concluding remarks

The OWCs deployed so far on the shoreline may be regarded as essentially demonstration prototypes and some are now employed as experimental infrastructures. The access on foot is easy and, at least for some of them, the special conditions at their location (including wave energy concentration effects) are not easily replicable elsewhere. Some of these plants and their equipment survived for many years (the Pico plant is still operational after 16 years) and demonstrated the survivability of their technologies under very harsh conditions.

The two most powerful wave energy devices constructed so far (the Osprey in UK and the greenWAVE in Australia, both rated 1 MW) were bottom-standing nearshore plants. Both were



Fig. 12. 100 kW shoreline OWC built in 2001 in Guangdong Province, China [27].



Fig. 13. Oceanlinx greenWAVE, Australia, rated power 1 MW. In Port Adelaide, before being towed to Port MacDonnell, 2014.

wrecked in disastrous deployment operations, in 1995 and 2014 respectively. This indicates that such operations are difficult and can be hazardous. The recent and successful deployment of the 500 kW bottom-standing OWC at Jeju Island, South Korea, shows that such difficulties can be overcome.

Integration into a breakwater is probably the easiest solution for

fixed-structure OWCs, from the economical, constructional and operational points of view. Naturally not all breakwaters are suitable for that, because of their type, location and orientation with respect to incident waves. The OWC breakwaters are being seriously considered for northern Spain (and not only at Basque Country) and for Italy (in spite of the low wave energy levels in the Mediterranean).

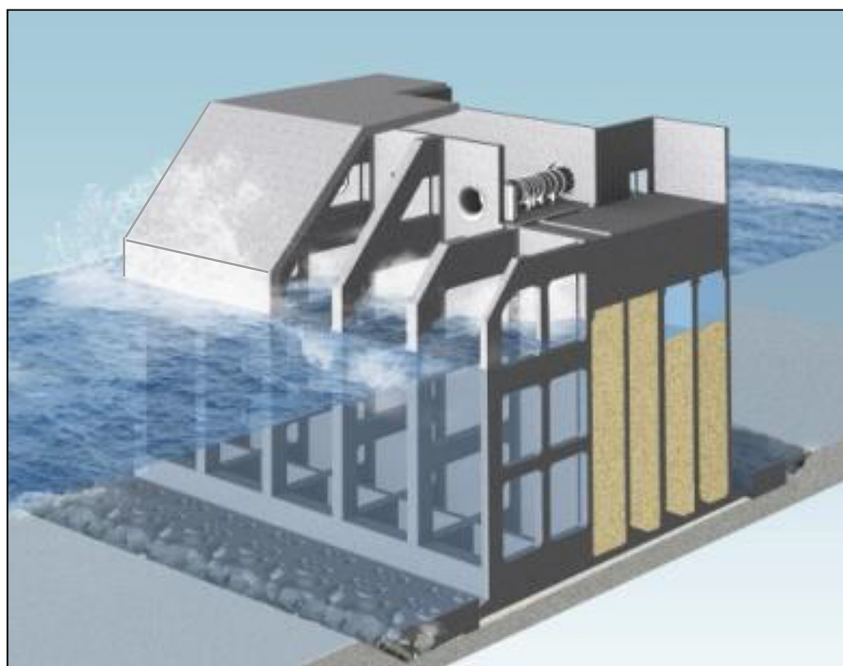


Fig. 14. 500 kW bottom-standing plant at Yongsoo, Jeju Island, South Korea, completed in 2015. Above: back view. Below: perspective section.



Fig. 15. Oceanlinx bottom-standing OWC, Australia, about 2005.

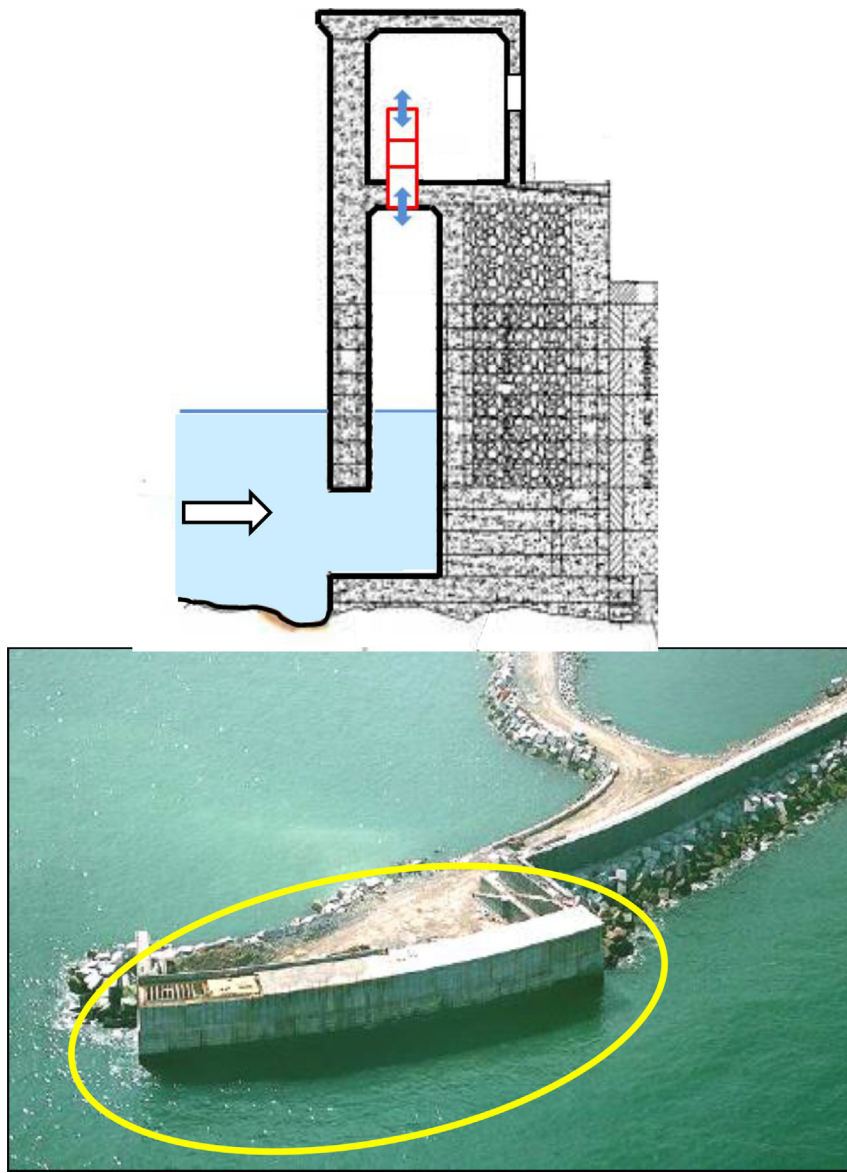


Fig. 16. Multi-chamber OWC plant integrated into a breakwater, Mutriku harbour, Basque Country, Spain, 2008–10.

As for floating oscillating-body devices, offshore OWCs have been proposed and developed with a wide range of configurations. The relative simplicity is their most obvious advantage. The OWC spar-buoy competes directly with vertical-axis two-body converters like the PowerBuoy, the water column playing the role of the inner body. Unlike the spar-buoy, the BBDB OWC and other small draught OWCs can be deployed into relatively shallow water, which may be an important advantage in some coastal regions like the South American Atlantic coasts.

Large floating structures with long rows of OWCs are being studied. From the viewpoint of energy production costs, they are possibly more expensive than dual-purpose OWC breakwaters, and their access for operation and maintenance is less easy. However, they exploit a more energetic resource offshore, and their location is not dependent on harbour protection convenience.

Converters with internal water column are at early stages of development. It is too soon for comparisons with more “conventional” OWC technologies. Having the air turbine protected from the corrosive and mechanical effects of sea water may be one of their advantages.

The hydrodynamic process of energy absorption from the waves by an OWC device is related to the interference between the incident wave field and the radiated waves produced by the motion of the body and/or the motion of the OWC. It can be said that a good wave energy absorber must be a good wave radiator. Obviously, in fixed-structure devices, the wave radiation is induced only by the water column motion. Almost the same can be said of OWCs mounted on a very large floating structure. The opposite happens with OWC spar-buoys if the bottom opening of the tube is more than say 40 m from the sea surface, and only the oscillating floater radiates waves. In devices, like the BBDB, the contributions from the structure motions and the water column oscillations are comparable, which may be regarded as a positive feature.

3. Air turbines

3.1. Introduction

More or less conventional unidirectional flow turbines (possibly Francis turbines or axial-flow turbines) can be used to equip OWCs

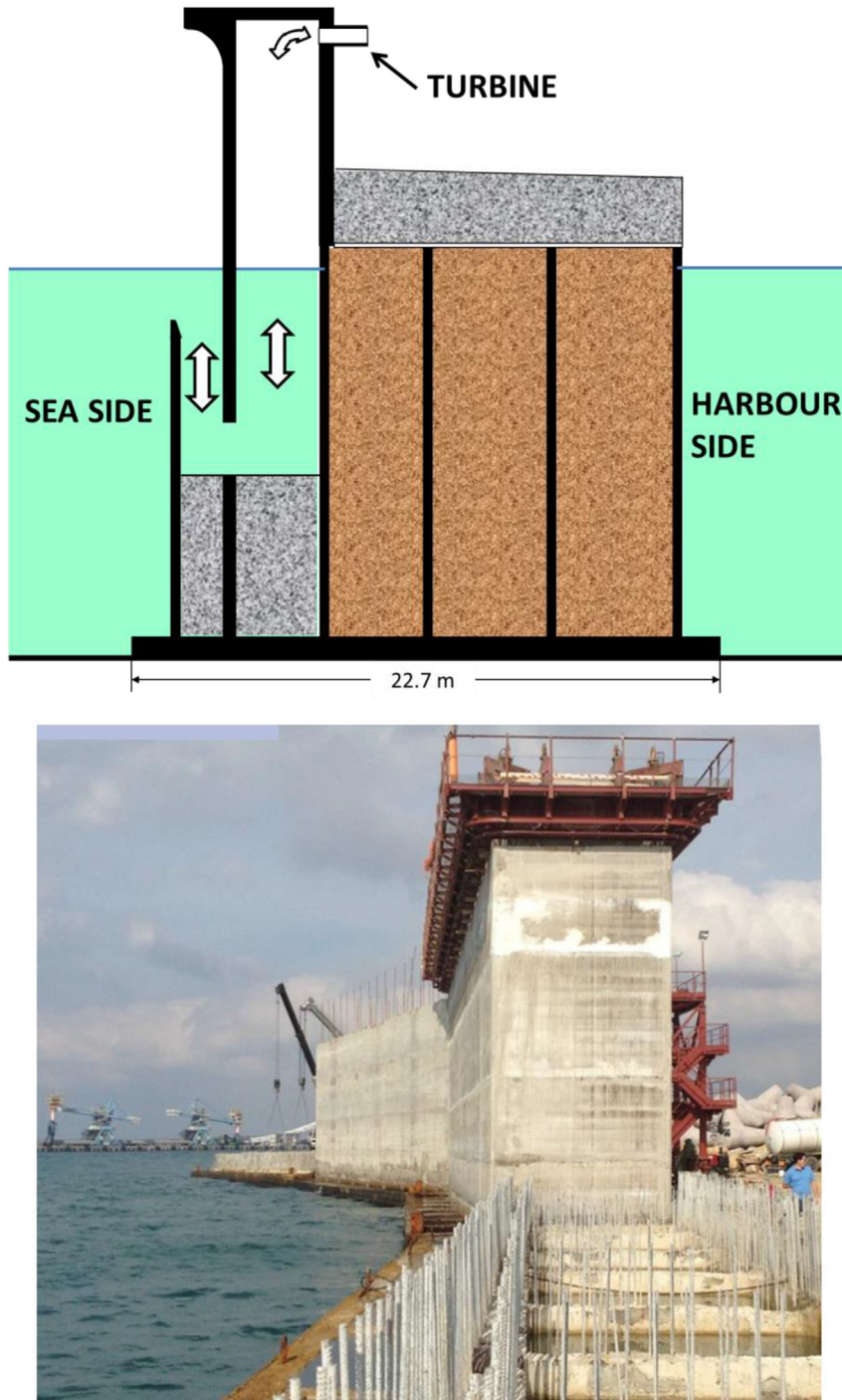


Fig. 17. Above: cross section of U-shaped OWC in a REWEC3 caisson breakwater for Civitavecchia harbour. Below: partly constructed breakwater at Civitavecchia harbour (2014).

provided that the wave energy converter is equipped with a rectifying system with non-return valves. Such systems were successfully used in small devices like navigation buoys [16] (Fig. 2). However, they have been regarded as unpractical in large plants, where flow rates may be of the order of $10^2 \text{ m}^3 \text{ s}^{-1}$ and the required response time is typically less than one second. This was confirmed by the experience with Kaimei [17]. Except for Kaimei and small navigation buoys, all (or almost all) OWC prototypes tested so far have been equipped with self-rectifying air turbines.

Most self-rectifying air turbines for wave energy conversion proposed and tested so far are axial-flow machines of two basic

types: the Wells turbine and the impulse turbine (other types will be mentioned later in this section). The Wells turbine was invented in 1976 by Dr Alan Arthur Wells (1924–2005) (at that time at Queen's University of Belfast, UK) [65] (Fig. 26). The most popular alternative to the Wells turbine is the self-rectifying impulse turbine, patented by Ivan A. Babintsev in 1975 [66]. Its rotor is basically identical to the rotor of a conventional single-stage steam turbine of axial-flow impulse type (the classical de Laval steam turbine patented in 1889 and developed in the 1890s and early 20th century by the pioneers of the steam turbine). Since the turbine flow is required to be bidirectional, there are two rows of guide vanes,



Fig. 18. 1:4th-scale prototype of BBDB (the OE Buoy) equipped with a Wells turbine being tested in Galway Bay, Ireland, about 2008.

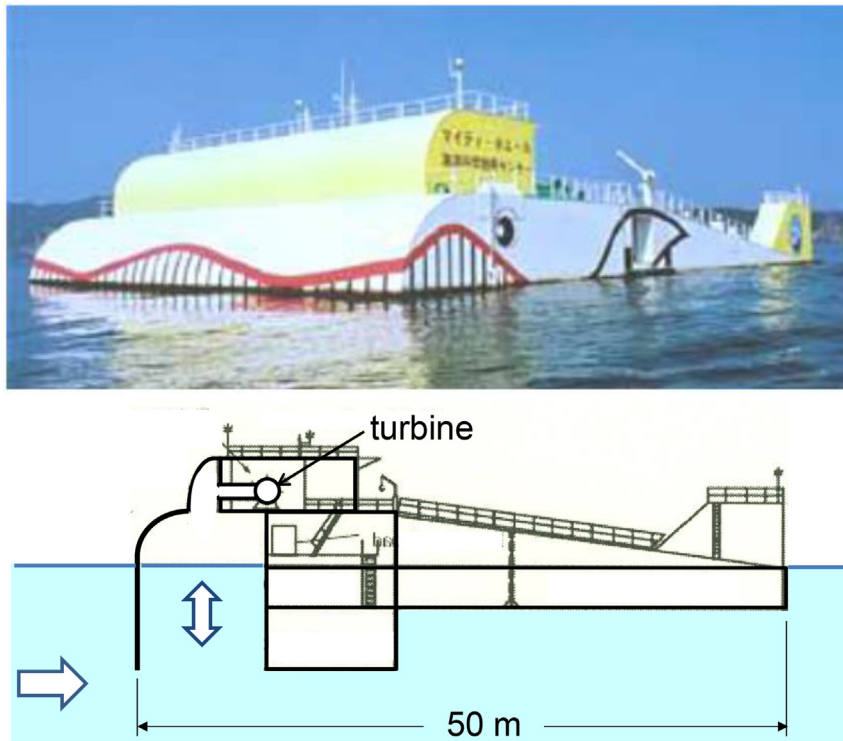


Fig. 19. Mighty Whale.

placed symmetrically on both sides of the rotor, instead of a single row (as in the conventional de Laval turbine). These two rows of guide vanes are like the mirror image of each other with respect to a plane through the rotor disc. The presence of guide vanes downstream of the rotor of an impulse turbine may introduce severe aerodynamic losses and is a major problem (see Section 3.3). Several versions of both types of turbines (Wells and impulse) have been proposed and tested, including the use of contra-rotating rotors (the McCormick contra-rotating turbine [47,67] is based on the impulse turbine concept).

A detailed review of Wells turbines was published in 1995 by Raghunathan [68]. For the impulse turbine see Ref. [69]. More recently, Setoguchi and Takao [10], Curran and Folley [11], Falcão and Gato [12] and Starzmann [13] published overviews on self-rectifying air turbines.

The so-called Euler turbomachinery equation relates the torque T_t , produced by the flow upon a turbine rotor, to the change in the flux of moment of momentum across the rotor [69]. If the one-dimensional approximation is adopted, we have more simply $T_t = \dot{m}(r_1 V_{t1} - r_2 V_{t2})$, where r is radial coordinate, V_t is tangential



Fig. 20. 1:3rd-scale Oceanlinx Mk3 multi-chamber floating OWC device, 2010.

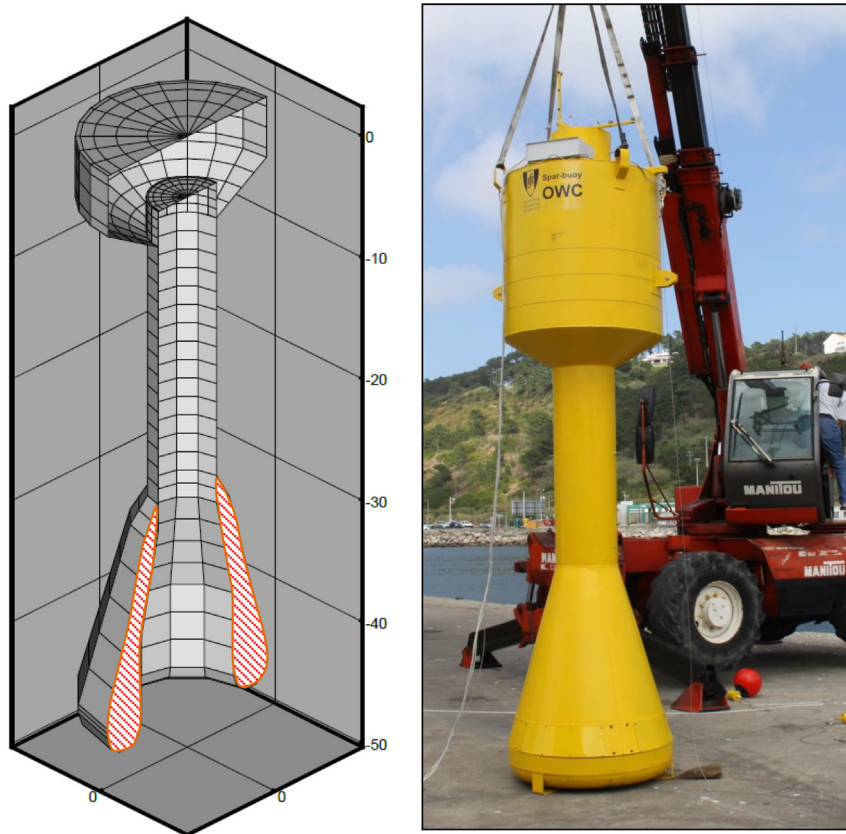


Fig. 21. Spar-buoy OWC. Cross section and 1:16th-scale model tested at NAREC, UK, in 2012.

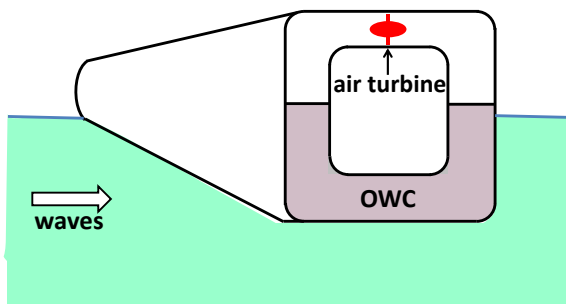


Fig. 22. Schematic representation of the U-Gen.

(or circumferential) component of the (absolute) flow velocity \mathbf{V} (positive in the direction of rotor blade motion), \dot{m} is mass flow rate, and subscripts 1 and 2 refer to the entrance to, and exit from, the rotor, respectively. This may be written as $E = \mathcal{Q} (r_1 V_{t1} - r_2 V_{t2})$, where $E = \mathcal{Q} T_t / \dot{m}$ is energy per unit mass of fluid and \mathcal{Q} is rotational speed (radians per unit time). For an axial-flow turbine rotor, with mean radius $r_1 = r_2 = r$, we have simply

$$E = \mathcal{Q} r (V_{t1} - V_{t2}). \quad (1)$$

This equation shows that the flow has to be deflected by the rotor blades in such a way that $V_{t1} > V_{t2}$. In conventional single-stage

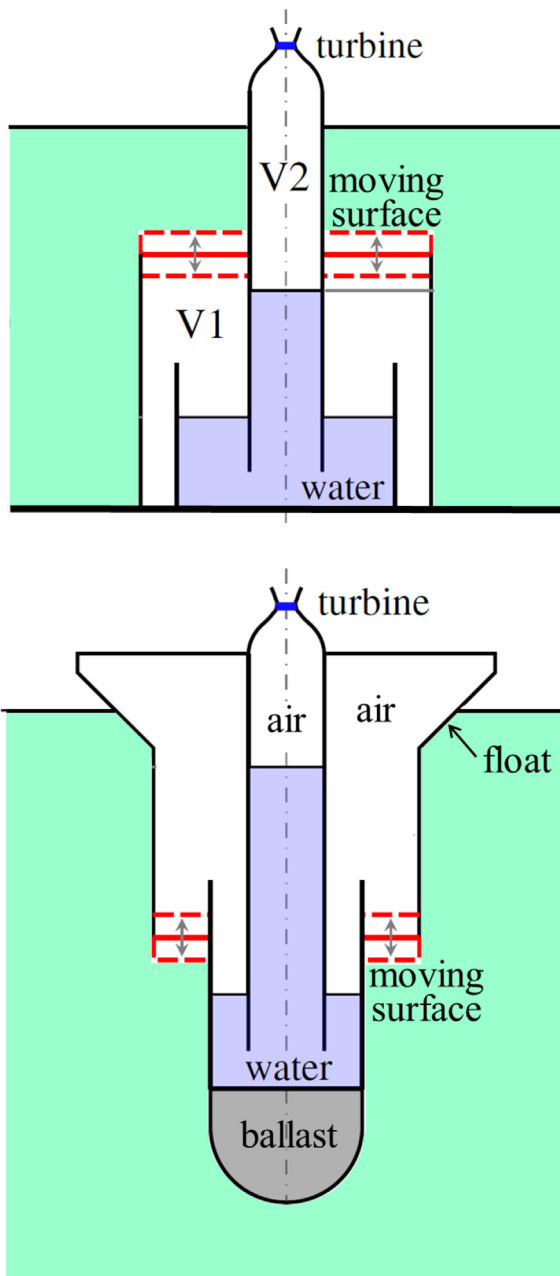


Fig. 23. Schematic representation of devices with compressible air volumes and water columns [57]. Above: sea-bottom standing version; below: floating version.

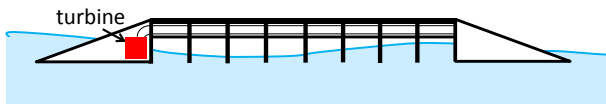


Fig. 24. Schematic representation of multi-OWC Seabreath.

axial-flow turbines like steam and gas turbines, the flow is deflected in a row of stationary blades upstream of the rotor in such a way that $V_{t1} > 0$ and, under design conditions, $V_{t2} \approx 0$. In this way, the swirl kinetic energy per unit mass $V_{t2}^2/2$, that is lost at the rotor exit, is minimized. This is especially important if, on the right-hand-side of Eq. (1), the blade velocity $\mathcal{Q} r$ is not much larger than $\Delta V_t = V_{t1} - V_{t2}$, as is the case of impulse turbines.

Because of construction reasons, open turbomachines, like horizontal-axis wind turbines and marine-current turbines, are not provided with guide vanes. On the other hand, the blade tip speed is much larger than ΔV_t (or than the axial velocity component), and the exit kinetic energy $V_{t2}^2/2$ is a small fraction of the work E . In the Wells turbine under normal working conditions, the rotor blade speed is also much larger than the flow velocity. For this reason, $V_{t2}^2/2$ is a relatively small fraction of the work E , and the absence of stator blades does not dramatically impair the turbine efficiency.

The cascade model is a convenient two-dimensional approximation to an axial-flow turbomachine: the blades are intersected by a circular cylindrical surface that is developed onto a plane. The three-dimension flow is replaced by a two-dimensional plane flow about a rectilinear periodic row, or cascade, of aerofoil profiles (see e.g. Ref. [69]). Equation (1) is replaced by

$$E = \mathcal{Q}rV_x(\cot \alpha_2 - \cot \alpha_1), \quad (2)$$

where V_x is the axial component of the flow velocity (assumed to take equal values upstream and downstream of the cascade) and $\cot \alpha_i = V_x/V_{ti}$ ($i = 1, 2$). The cascade approximation will be used in Sections 3.2 and 3.3 in the introductory study of the flow through Wells and axial-flow impulse turbines.

3.2. Wells turbines

We consider now the special case of the Wells turbine (without and with guide vanes), and the corresponding cascades and velocity diagrams (Fig. 27). The absolute flow velocity, relative flow velocity and rotor blade velocity are denoted by vectors \mathbf{V} , \mathbf{W} and \mathbf{U} , respectively (with $U = \mathcal{Q}r$). The rotor blade profile is symmetrical and the blades are set at a stagger angle of 90° (i.e. they are symmetrical with respect to a plane perpendicular to the rotor axis). Early theoretical investigations on the Wells turbine aerodynamics, based on the two-dimensional cascade flow model, are reported in Refs. [70–72] (Fig. 27).

We consider the two-dimensional cascade flow approximation, and denote by c the rotor blade chord and by $t = 2\pi r/Z$ (Z = number of blades) the rotor blade pitch. Before dealing with real fluid flow, we derive some remarkable aerodynamic properties of the Wells turbine from well-known analytical results for a cascade of flat plates in incompressible irrotational flow [73–75] (see also [12]). For that, as an approximation, we assume incompressible irrotational flow and neglect the blade thickness. We find (see Ref. [76])

$$\cot \alpha_2 = \cot \alpha_1 + 2 \tan \frac{\pi c}{2t}. \quad (3)$$

From Eq. (2), we directly obtain, for the rotor work per unit mass of air,

$$E = 2\mathcal{Q}rV_x \tan \frac{\pi c}{2t}. \quad (4)$$

Equation (3) shows that the exit flow angle α_2 depends only on α_1 and on the rotor chord-to-pitch ratio c/t , not on the flow rate or on the rotational speed. This is the basis of the design of guide vanes for a Wells turbine. If the two rows of guide vanes are to be the mirror image of each other, it should be $\alpha_2 = \pi - \alpha_1$. Then

$$\alpha_1 = \frac{\pi}{2} \left(1 + \frac{c}{t} \right) \quad (5)$$

is the angle at which the flow should leave the first row of guide vanes [80]. It is important to relate the pressure drop Δp to the flow rate. We define a dimensionless pressure coefficient $\psi = \Delta p (\rho \mathcal{Q}^2 r^2)^{-1}$ (ρ = air density) and a dimensionless flow rate

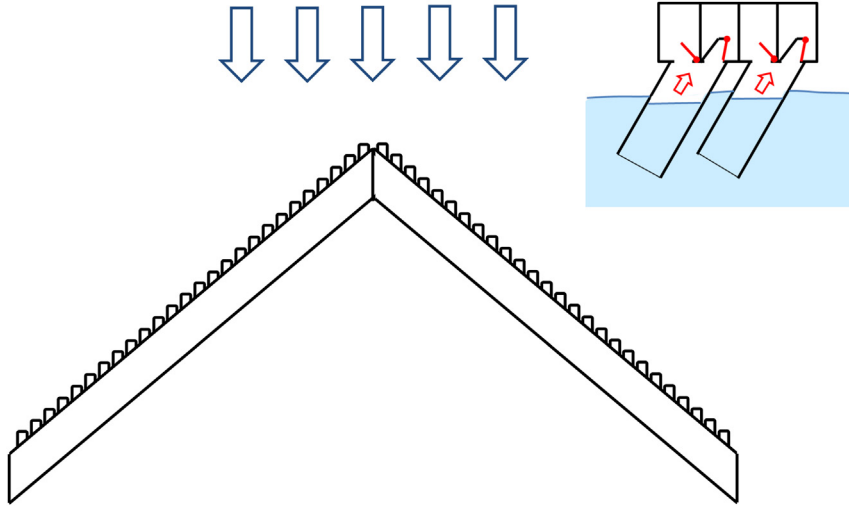


Fig. 25. Schematic representation of multi-OWC LEANCON.



Fig. 26. Dr Alan Arthur Wells, inventor of the Wells turbine (1924–2005).

coefficient $\phi = V_x \Omega^{-1} r^{-1}$. Assuming as before perfect-fluid flow, it can be found for a Wells turbine cascade with guide vanes [12,76]

$$\psi = 2\phi \tan \frac{\pi c}{2t}. \quad (6)$$

In the case of a Wells turbine without guide vanes, Eq. (6) is replaced by (see Ref. [12])

$$\psi = 2\phi \left(1 + \phi \tan \frac{\pi c}{2t}\right) \tan \frac{\pi c}{2t}. \quad (7)$$

Equation (6), applicable to a Wells turbine with guide vanes, is a linear relationship between pressure and flow rate. The slope of the straight line increases with the rotor blade-chord-to-pitch ratio c/t . In the case of a Wells turbine without guide vanes (see Eq. (7)), the linear relationship is an approximation, since in general $\phi \tan(\pi c/2t)$ is much smaller than unity. This linear relationship is approximately confirmed by results from model testing. Indeed, unlike other self-rectifying turbines, the Wells turbine is commonly regarded as a linear turbine.

Apart from two rows of guide vanes one on each side of the rotor, there are other ways of avoiding exit losses due to swirling flow, while keeping the turbine insensitive to reversing flow direction. One of them is the contra-rotating turbine without guide vanes: there are two rows of rotor blades (with identical profile and blade pitch) that rotate in opposite directions with equal speed, as shown in Fig. 28. For the whole turbine it is

$$\psi_1 + \psi_2 = 4\phi \tan \frac{\pi c}{2t}. \quad (8)$$

and $E = E_1 + E_2$, with $E_1 = E_2$ given by the right-hand-side of Eq. (4).

The work per unit mass E done by a rotor with a single row of blades increases with the chord-to-pitch ratio c/t , as shown by Eq. (4). Obviously this ratio cannot be too close to unity. The contra-rotating rotor configuration provides a way of doubling the work E . A major disadvantage is the increased complexity due to two turbine-generator rotating sets and the duplication of the power electronics. An alternative way is to have two axially-offset rows of rotor blades mounted on a single rotor (biplane rotor). As the original monoplane Wells turbine, the biplane Wells turbine originated also at the Queen's University of Belfast [77] where it was object of investigations whose results are reported in detail in Raghunathan's review paper [68]. The biplane rotor can be complemented or not by guide vanes on both sides of the rotating blade set (see Ref. [12]). Biplane Wells turbines without guide vanes were used in the cliff-integrated Islay OWC plant commissioned in 1995 [20] and, more recently, in the Mutriku OWC breakwater [31]. A different configuration, proposed in Ref. [78], consists in placing the guide vanes between the two rotor blade rows. If properly designed (see Ref. [12]), this arrangement can provide a way of avoiding or minimizing swirl kinetic energy losses at turbine exit. It can also be extended to more than two rotor blade planes, in what could be considered as a multi-stage turbine. Multistage Wells turbines were investigated as an alternative to impulse turbines in OWCs characterized by relatively large air pressure oscillations [79].

In linear (small amplitude) water wave theory, the wave crests and troughs are of similar amplitude and so the predicted air flow velocities through the turbine are of identical magnitudes in both directions. However, this is not true for real sea waves, especially in more energetic sea states. The wave crests tend to be higher and shorter as compared with the wave troughs. Consequently the flow conditions through the air turbine may be significantly different, with peak velocities for outward flow in general larger than for inward flow. In order to equalize the peak values of the angle of incidence at the inlet to rotor blades in inward and outward flows (and avoid stalling losses due to excessive incidence), a stagger angle (slightly) different from 90° may be adopted, as proposed in Refs. [80,81].

Turbines whose rotor blade setting angle (stagger angle) is adjustable and controllable have been proposed and built. A

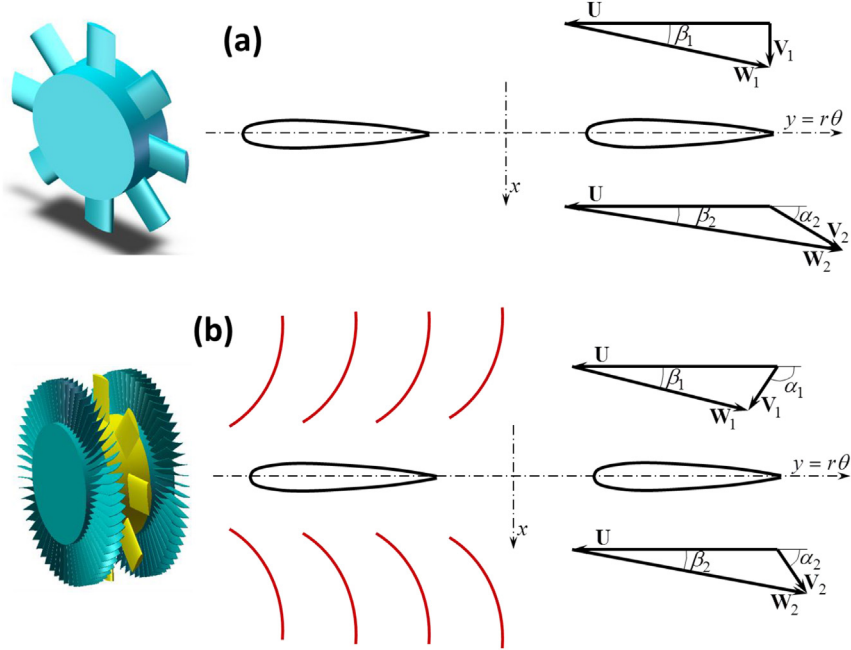


Fig. 27. Wells turbine, two-dimensional cascade representation and velocity diagrams: (a) without guide vanes; (b) with guide vanes.

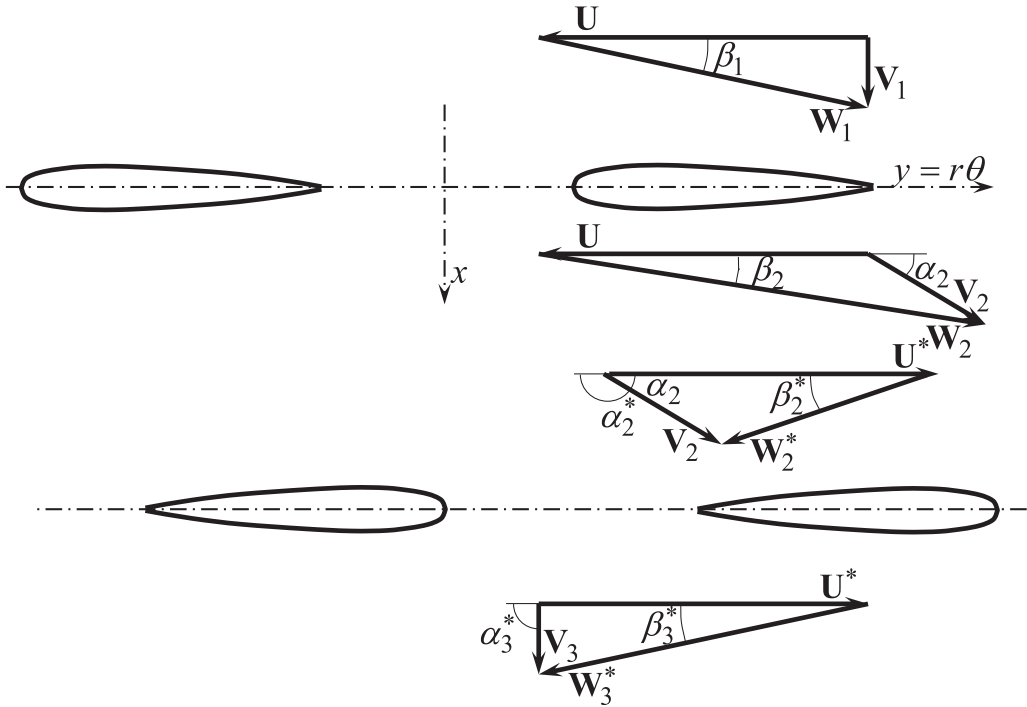


Fig. 28. Two-dimensional cascade representation of the Wells turbine with two contra-rotating rotors.

400 kW variable-pitch Wells turbine, whose sophisticated control mechanism was driven by eddy currents was designed and constructed [82], Fig. 29. This will be mentioned again in Section 5.1 in connection with reactive control.

3.3. Axial-flow self-rectifying impulse turbine

The most frequently proposed alternative to the Wells turbine is

the axial-flow self-rectifying impulse turbine (Fig. 30). In the impulse turbine (unlike in the Wells turbine), neighbouring rotor blades form channels or ducts. The exit flow angle (in a reference frame fixed to the blade row) is approximately equal to the exit angle of the (moving or fixed) blades (the angular difference corresponding to the effect of slip).

The geometry of the rotor blades is a modified version of the classical steam turbine of impulse type (see e.g. Ref. [69]): the

symmetry now imposes two sharp edges and equal inlet and outlet blade angles. As for the Wells turbine, we replace the three-dimensional annular row of rotor blades by the corresponding two-dimensional cascade of blades (Fig. 30) and assume the flow to be incompressible and irrotational. We denote by α and β the angles of the absolute and relative flow velocities. Those angles (at inlet and outlet) are related to each other by $\cot\alpha_1 = -\phi^{-1} + \cot\beta_1$, $\cot\alpha_2 = -\phi^{-1} + \cot\beta_2$, where, as before, $\phi = V_x/U$ is a dimensionless flow coefficient and V_x is the axial velocity component. We note that $\alpha_1 > \beta_1$ and $\alpha_2 > \beta_2$. Fig. 30 shows that, under design conditions, the flow leaves the rotor at an angle α_2 significantly larger than $\pi - \alpha_1$, where α_1 is the exit flow angle from the inlet guide-vane row. We note that symmetry considerations require a second guide-vane row to exist, which is the mirror image of the first one. The “ideal” inlet flow angle into this guide-vane system (i.e. for stall-free conditions) is equal to $\pi - \alpha_1$. However, for “design” flow conditions, this cannot occur. An incompatibility situation arises from this: one cannot have simultaneously the right flow incidence (i.e. stall-free conditions) at the rotor blades and at the second guide-vane row, a problem that has been known since the beginning to designers of impulse turbines for wave energy applications.

McCormick [47,83] proposed a contra-rotating self-rectifying impulse turbine, a prototype of which was built and tested in Kaime in the mid-1980s. Results from testing can be found in Ref. [83]. The excessive incidence problem persists in the contra-rotating turbine, in the relative flow at the inlet to the second rotor, and (as in the single-rotor turbine) also in the flow at the inlet to the second row of guide vanes.

To solve the excessive incidence problem, guide vanes of variable geometry have been proposed by Kim et al. [84] (see also a review in Ref. [9]). In order to avoid the difficulties of active geometry-control, the vanes (or a segment of them) may pivot under the action of the aerodynamic moments acting on them, and occupy one of two pre-set angular positions, depending on whether the air is flowing inwards or outwards (Fig. 31). This allows the downstream guide-vane geometry to better match the angle α_2 of the flow leaving the rotor. Although this conception increases the mechanical complexity and introduces additional reliability and maintenance problems, it has been found to improve the aerodynamic performance of the turbine.

In any case, since the flow coefficient ϕ is strongly time-varying, oscillating irregularly between negative and positive values, it is impossible to avoid aerodynamic stalling at the rotor blades and/or at the downstream guide vanes during a relatively large part of the time.

3.4. Wells turbine versus axial-flow impulse turbine

The operating flow range of a Wells turbine is known to be relatively narrow: for increasing flow rate, the efficiency drops sharply when stalling at rotor blades occurs [10–12,68]. For the best designs, peak efficiency under laboratory conditions was found to reach about 75% [13].

The main problem with the impulse turbine lies in the large aerodynamic losses due to excessive incidence flow angle at the entry to the second row of guide vanes (this is a result of the required symmetry of the guide vane rows with respect to each other). Although the operational flow range of the impulse turbine is wider compared with the Wells turbine, its peak efficiency hardly exceeds about 50%. To reduce these losses, guide vanes of variable geometry have been proposed (see Section 3.3). This was found to increase the peak aerodynamic performance of the turbine up to about 60%. A comparison of the efficiency-versus-flow-rate curves of the two types of turbines is shown in Fig. 32.

The two-dimensional representation may be used to make comparisons between rotational speed, basic aerodynamic performance

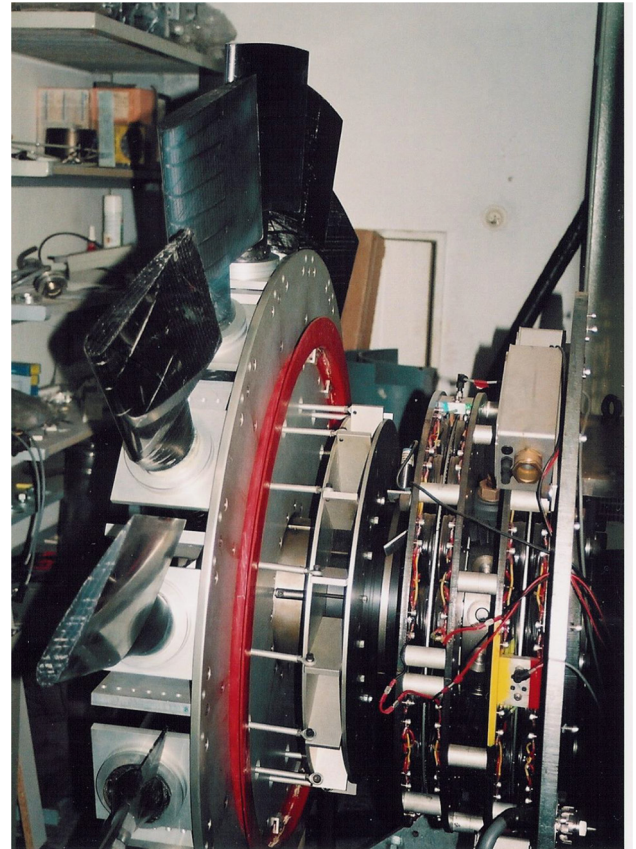


Fig. 29. 400 kW variable-pitch Wells turbine built for installation at the Pico plant. The control mechanism is driven by eddy currents.

and rotor diameter of the Wells turbine and of the impulse turbine. We start by considering the dimensionless turbine loading coefficient, defined as $E^* = E(\Omega r)^{-2}$. For the Wells turbine (subscript W) with a single-plane rotor, with or without guide vanes, it is (see Eq. (4))

$$E_W^* = 2 \frac{V_x}{\Omega r} \tan(\pi c/2t). \quad (9)$$

We note that, in the absence of guide vanes, it is $\phi = V_x(\Omega r)^{-1} = \tan\beta_1$. In real-fluid flow, it is known that aerodynamic stalling (boundary layer separation) will occur (with severe aerodynamic losses) if the angle of incidence β_1 at rotor inlet exceeds a critical value $\beta_{1\text{cr}}$ that depends on blade profile, chord-to-pitch ratio c/t , upstream flow conditions and Reynolds number. Taking $\beta_1 = \beta_{1\text{cr}}$, and assuming as typical $\beta_{1\text{cr}} = 11^\circ$ and $c/t = 0.5$, we find, for the loading coefficient, $E_W^* \approx 0.39$. For the impulse turbine (subscript “imp”), from similar considerations [12], it can be found that $E_{\text{imp}}^* \approx 2.0$. We conclude that, for fixed work E per unit mass, the blade speed Ωr of the Wells turbine is typically about $\sqrt{2.0/0.39} = 2.3$ times larger as compared with the impulse turbine.

The two-dimensional flow approximation was used in Ref. [12] to compare the Wells turbine (subscript W) and the axial-flow impulse turbine (subscript imp), it being assumed that the work E per unit mass, the turbine flow rate and the inner/outer diameter ratio D_i/D are equal for both turbines. The results are given in Table 1, in terms of ratios, for V_x^2 (twice the exit kinetic energy per unit mass), the rotor outer diameter D and the rotational speed Ω . Table 1 shows that the rotor blade speed is much larger in a Wells turbine, which also has a larger diameter and larger rotational speed. This indicates that aerodynamic noise problems are

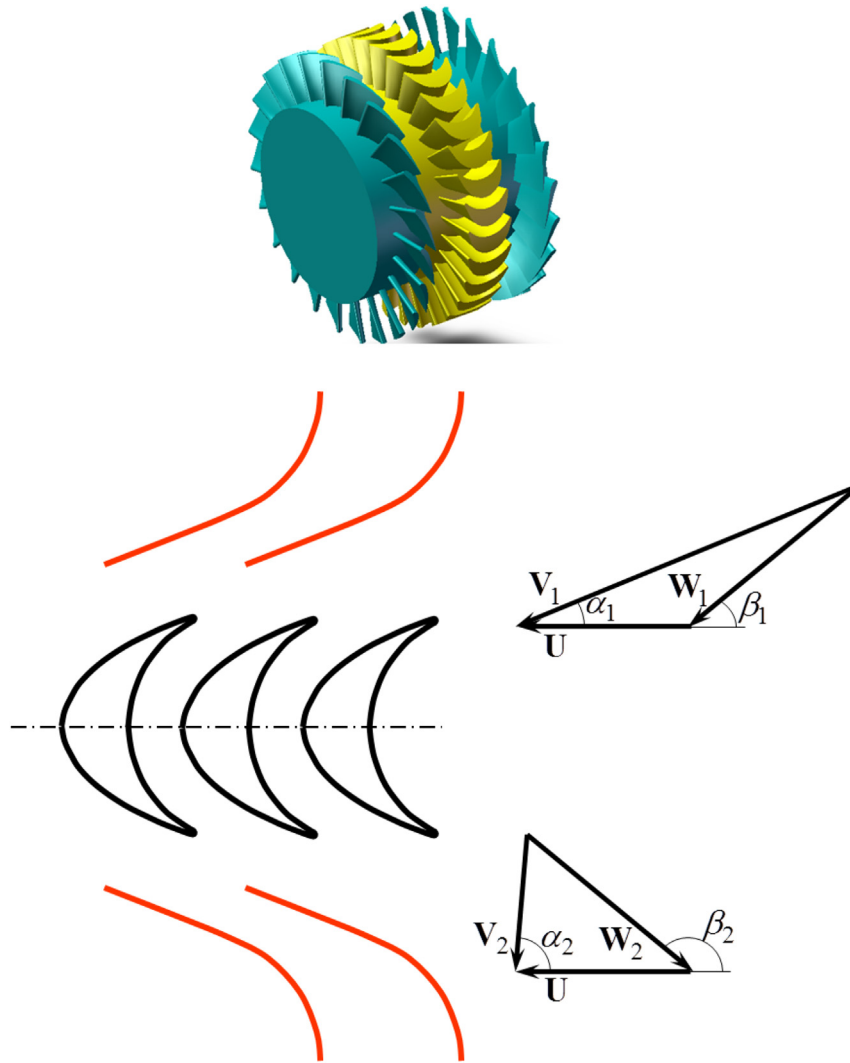


Fig. 30. Self-rectifying impulse turbine: rotor with twin guide vane system. Below: two-dimensional cascade representation.

expected to be much more serious in the Wells turbine (see Section 3.8), which, on the other hand, has a much larger capacity for energy storage by flywheel effect (this is important to smooth out the power oscillations in the electrical equipment).

The loss related to swirl kinetic energy at the exit from the last row of blades can be avoided (or reduced) by the use of guide vanes or (in the case of the Wells turbine) of contra-rotating rotors. The loss of the kinetic energy (per unit mass) associated to the axial flow velocity, $V_x^2/2$, cannot be avoided except if some kind of, possibly axisymmetric, divergent duct is used as a diffuser. This loss is much greater in the impulse turbine than the Wells turbine, as shown in the first column of Table 1. This explains why the use of an axisymmetric diffuser is much more important in an impulse turbine than in a Wells turbine.

The two-dimensional flow analysis indicates that the efficiency of the Wells turbine can be much more sensitive to changes in Reynolds number than the efficiency of the impulse turbine [12]. The Wells turbine is known to perform poorly in small model testing (and small flow velocities), more so than the impulse turbine, mostly due to Reynolds number effects. A fair comparison between the two turbines should be based on results from testing at sufficiently large Reynolds number. Some of the comparisons in

the published literature that show the Wells turbine with substantially lower peak efficiency than the impulse turbine are based on testing of models of 0.3 m outer rotor diameter or less at relatively small Reynolds number.

3.5. Other axial-flow air turbines for bidirectional flows

An alternative method of reducing the aerodynamic losses by excessive incidence angle at the entrance to the second row of guide vanes of an impulse turbine consists in increasing the distance between the guide vane rows and the rotor blades, with the object of reducing the velocity (and hence the kinetic energy) of the flow at the entrance to the second row of guide vanes and in this way reduce the energy losses due to boundary layer separation (stalling) at those vanes. This methodology was proposed in Refs. [85,86]: the two rows of guide vanes, one on each side of the rotor, are offset from the rotor blades, radially as well as axially, with annular ducts connecting the guide vane sets with the rotor blade row. The radial offset allows, by conservation of angular momentum, the circumferential component of the flow velocity to be reduced at the entrance to the second row of guide vanes. This radial offset, eventually combined with an increase in the gap

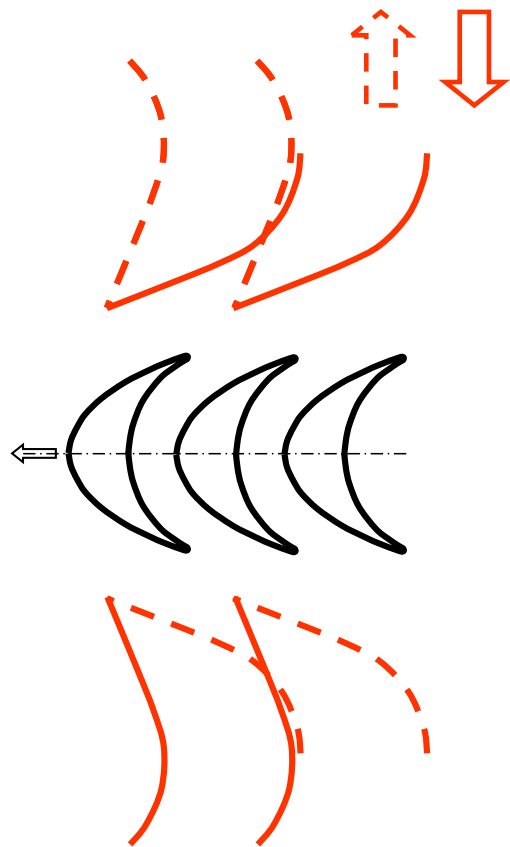


Fig. 31. Two-dimensional representation of impulse turbine with self-pitching guide vanes (of mono-vane type) in the two angular positions.

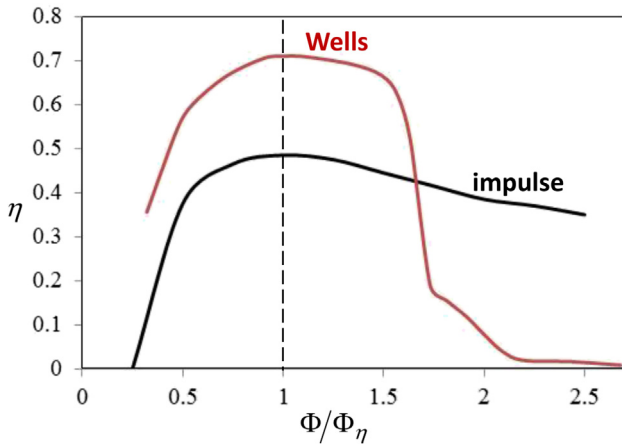


Fig. 32. Efficiency versus flow coefficient ratio Φ/Φ_η for a monoplane Wells turbine with guide vanes and an impulse turbine with fixed guide vanes. Φ_η denotes peak efficiency conditions. From Ref. [12].

between the inner and outer walls of the annular ducts (i.e. an increase in blade span of the stator system), produces also a decrease in the meridian component (projected onto an axial plane) of the flow velocity. One such turbine, commercially named HydroAir (Fig. 33), equipped the 1:3rd-scale floating OWC prototype Oceanlinx Mk3 briefly tested off Port Kembla, Australia, in 2010 (see Fig. 20).

The so-called Denniss-Auld turbine, developed in Australia to equip OWC plants [87,88], is a self-rectifying axial-flow turbine,

that shares some characteristics with the variable-pitch Wells turbine, the main difference being that the setting angle γ of the Denniss-Auld rotor blades (Fig. 34) may be controlled to vary within a range $\alpha < \gamma < \pi - \alpha$ (where $\alpha \approx 20 - 35^\circ$), whereas in the variable-pitch Wells turbine it is $-\theta < \gamma < \theta$ (with $\theta \approx 25^\circ$). While in the Wells turbine the rotor blade rounded leading edge faces the incoming flow all the time, in the Denniss-Auld turbine both edges of a blade must be identical since (like in the impulse turbine rotor) each edge behaves alternately as a leading edge or as a trailing edge depending on the direction of the reciprocating flow through the turbine. It is to be noted that, whenever the flow changes direction (exhaust or intake), the blades of the Denniss-Auld turbine are required to pivot almost instantaneously between their extreme positions, whereas in the Wells turbine the blades are required to pivot smoothly within a relatively small angular range. Results from model testing gave a peak efficiency of 0.65 [88]. A Dennis-Auld turbine prototype was tested in Oceanlinx Mk3 side-by-side with the HydroAir turbine (Fig. 20).

3.6. Radial-flow self-rectifying air turbines

Apart from the more common axial-flow configuration, studies have also been made on radial-flow self-rectifying impulse turbines (Fig. 35). It should be noted that the turbine is no longer insensitive to the flow direction: the flow through the rotor blades and guide vanes is radially centrifugal or centripetal depending on the wave cycle. The turbine is connected to the OWC chamber by an axial duct, whereas the exit to, or admission from, the atmosphere is radial. The radial turbine was investigated by model testing [89–91] and by numerical simulation [92–95]. Takao et al. [96] investigated the effect of pitch-controlled (inner and outer) guide vanes, and found an increase up to about 15% in the efficiency in comparison with fixed guide vanes. With the available (experimental and numerical) information, the radial configuration of the impulse turbine appears as an alternative to the axial one, although not necessarily a better choice.

A radial-flow version of the classical axial-flow Wells turbine was proposed by John Kentfield in 1983 [97], and was recently studied by numerical simulation and experimentally [98,99] (Fig. 36). The results from model testing revealed that, as for the more conventional axial-flow Wells turbine, the pressure head is approximately a linear function of the flow rate, and a sharp drop in efficiency occurs if the flow rate exceeds a critical value; this value is about 30% higher for outward flow. A peak efficiency of 0.65 was measured for outward flow, compared with 0.60 for inward flow.

A different type of self-rectifying radial-flow turbine, that was patented [100] and model tested [101], has a pair of guide-vane rows mounted on the periphery of the radial-flow rotor. The guide-vane row pair slides axially, by gravity and aerodynamic action, so as to convert the bidirectional flow admitted to the turbine into unidirectional flow through the rotor, as shown in Fig. 37. Experimental results are reported in Ref. [101] for different guide-vane setting angles. The maximum measured peak efficiency was about 57%. The turbine performance seems to be penalized by the

Table 1

Comparison between typical Wells (W) and impulse (imp) turbines. Ratios are shown for axial flow velocity V_x , outer rotor diameter D and rotational speed Ω . The work per unit mass E , the flow rate and the inner-to-outer diameter ratio D_i/D are the same for both turbines.

$\frac{V_x^2}{V_x^2_{imp}}$	$\frac{D_W}{D_{imp}}$	$\frac{\Omega_W}{\Omega_{imp}}$
0.27	1.4	1.7

lack of an efficient diffusor system for the recovery of kinetic energy at rotor exit.

The so-called biradial turbine [102–104] is an impulse turbine that is symmetrical with respect to a plane perpendicular to its axis of rotation (Fig. 38). The flow into, and out of, the rotor is radial. The rotor is surrounded by a pair of radial-flow guide-vane rows, each row being connected to the corresponding rotor inlet/outlet by a duct whose walls are flat discs. In version 1, as a way of reducing the losses due to excessive incidence at the entry to the second row of guide vanes, the guide vanes are radially offset from the rotor (Fig. 38b). This allows the exit flow from the rotor to be decelerated in the connecting duct (both the circumferential and radial velocity components are decreased) which results in smaller aerodynamic stall losses at the guide vanes. Alternately, in version 2, the guide vane rows may be removed from, or inserted into, the flow space by axially displacing the whole guide vane set, so that the downstream guide vanes are prevented from obstructing the flow coming out of the rotor. In this case, the radial distance between the rotor and the guide vanes is small, as shown in Fig. 38a. The biradial turbine was studied by numerical simulation [103] and model testing [104]. The measured peak efficiency of version 2 was about 79%, possibly the highest efficiency of a self-rectifying air turbine measured so far.

Single stage conventional turbines, like steam and gas turbines, with a row of guide vanes followed by a bladed rotor, are known to attain high efficiencies in unidirectional flow. In such turbines, if the sign of the pressure head is changed (and the rotational speed is kept unaltered), the flow rate (apart from changing sign) becomes much smaller (and the turbine performance becomes very poor). This has led to the idea of associating two identical “conventional” air turbines (turbines T1 and T2) in parallel to convert the



Fig. 33. HydroAir turbine.

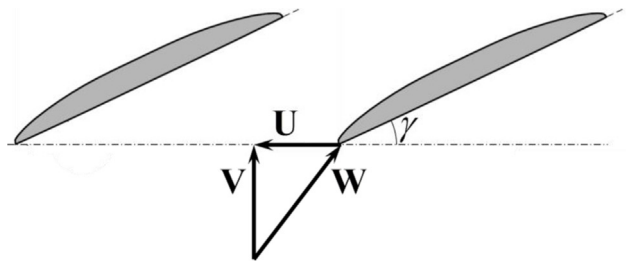


Fig. 34. Denniss-Auld turbine. Below: velocity diagram and blade setting angle γ .

pneumatic energy from an OWC, such that, for a given pressure head situation, the flow sequence guide-vanes-rotor-blades in turbine T1 is reversed with respect to turbine T2 (see Refs. [105–107]). This topology is shown in Fig. 39. With this arrangement, for a given pressure head (independently of its sign), most of the flow is admitted to one of the turbines (that is driven with good efficiency) while a smaller fraction of the flow is admitted to the other turbine (that is in choking mode and operates at very low efficiency). The two turbines can be coupled to a common electrical generator (as in Fig. 39) or, alternately, each turbine is coupled to its own generator. Since the turbines are not symmetrical, their rotor blades, as in Fig. 39, need no longer to be symmetrical with respect to the mid-chord point. Some positive degree of reaction may be convenient. Model testing of a unidirectional-turbine pair in a rig capable of bi-directional oscillating air flow is reported in Ref. [106]. The turbine rotor diameter was 165 mm and each turbine was coupled to its own generator. A peak efficiency of 0.6 was measured. The aerodynamic performance of the twin unidirectional turbine configuration was numerically simulated in detail in Ref. [108]. It was found that the flow rate through the turbine in reverse mode is about one-third of the total flow and produces a negative torque which reduces the system efficiency if the two turbines are directly connected to the same rotation axis.

3.7. Some air turbine prototypes

Several full-sized OWC prototypes have been deployed into the sea; in some cases large models at scales about 1:3rd to 1:4th have

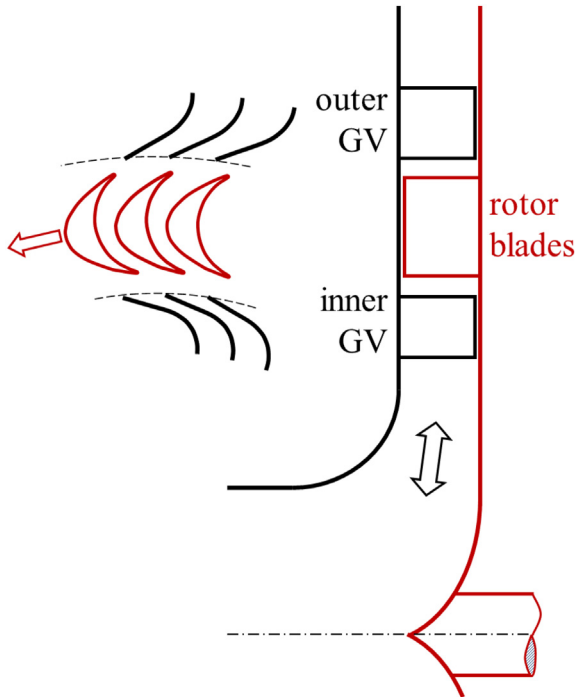


Fig. 35. Schematic representation of the radial self-rectifying impulse turbine.

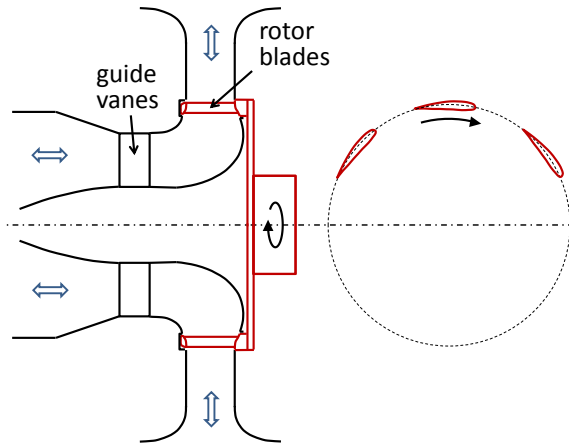


Fig. 36. Radial-flow version of the Wells turbine.

been tested in sheltered waters. The first large prototype was Kai-me, already mentioned in Section 2.1, in whose thirteen open-bottom chambers different types of turbines were tested (including unidirectional, Wells and self-rectifying impulse turbines). Since then, most prototypes were equipped with Wells turbines, some of which are listed in Table 2, together with their main characteristics. Remarkable for their size are the pair of 2×500 kW contra-rotating Wells turbines that equipped the bottom-standing OSPREY prototype (Fig. 40). They never operated: the plant structure was damaged during deployment in Scotland in 1995 and later destroyed by wave action.

The Indian bottom-standing OWC plant, commissioned in 1991, was operated with several axial-flow self-rectifying air turbines of Wells and impulse type [24]. The Mutriku plant recently completed in northern Spain (Fig. 15) comprises 16 OWC chambers, each equipped with a 0.75 m-diameter vertical axis Wells turbine of

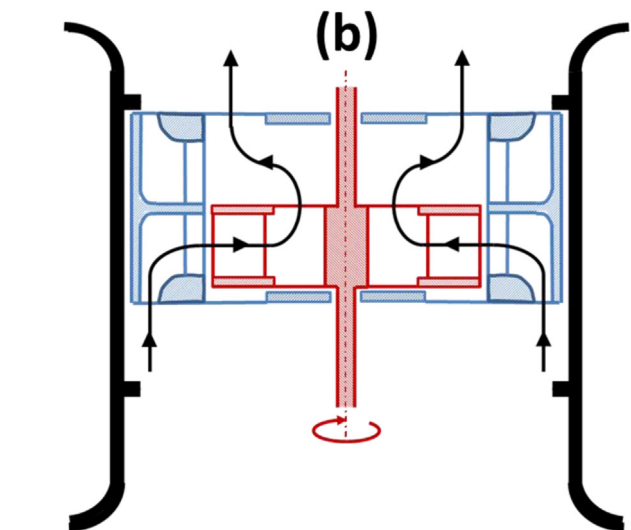
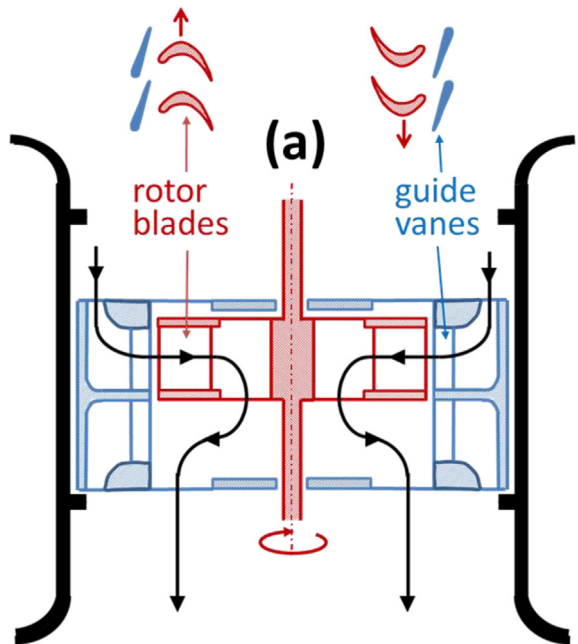


Fig. 37. Self-rectifying radial-flow turbine with unidirectional-flow rotor and twin axially sliding guide-vane rows. Guide vane position: (a) for downward flow; (b) for upward flow.

biplane type without guide vanes, rated 18.5 kW [31,113]. The Dennis-Auld turbine equipped the several OWC prototypes Mk1 (bottom standing) to Mk3 (floating), developed in Australia. The prototype Mk 3 (1:3rd scale), briefly tested in 2010, also incorporated a HydroAir impulse turbine (Figs. 20 and 33). The 1:4th-scale BBDB OWC (the OE Buoy) tested in Galway Bay, Ireland, between 2008 and 2011 (Fig. 18) was equipped first with a Wells turbine and later with an axial-flow self-rectifying impulse turbine with actuated variable-pitch guide vanes [41,42], Fig. 41. The recently completed bottom-standing OWC, located at Juju Island, South Korea (Fig. 14), is equipped with two 250 kW axial-flow impulse turbines of 1.8 m diameter, with 26 rotor blades and fixed guide vanes (Fig. 42).

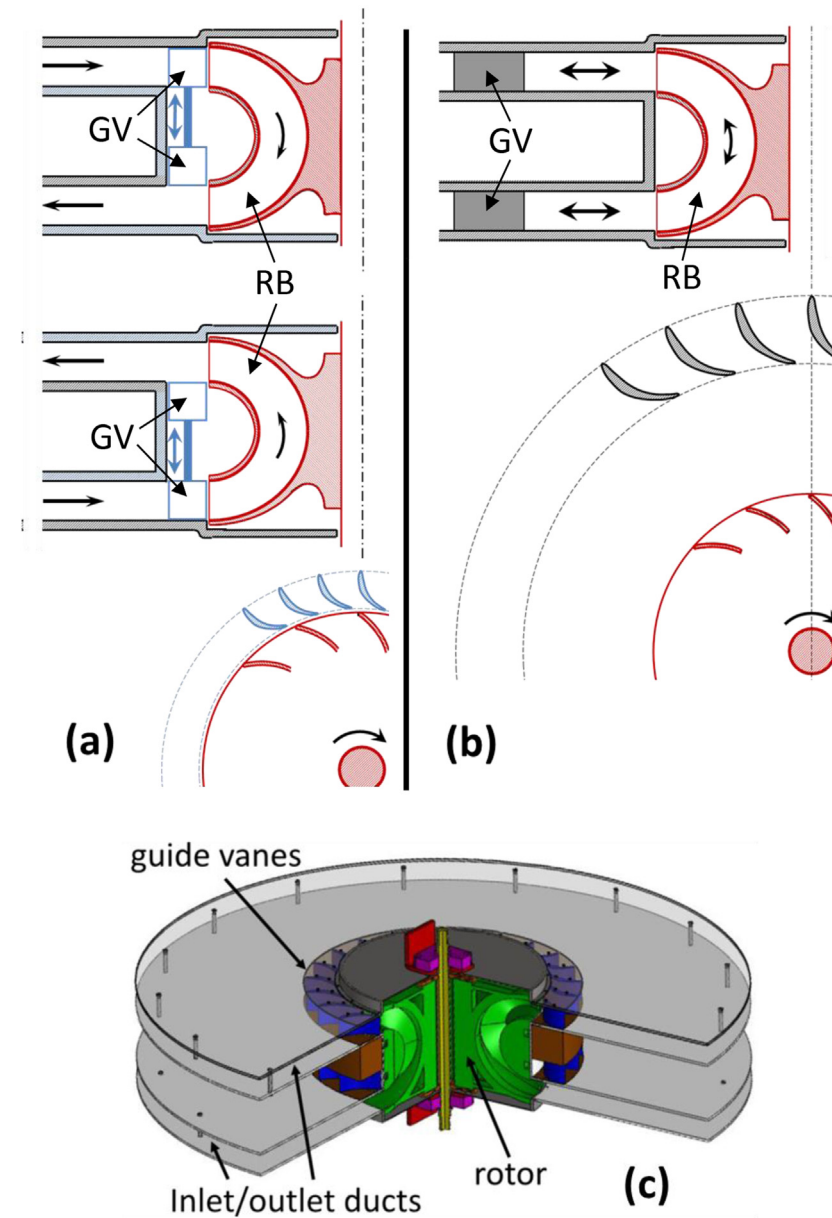


Fig. 38. Biradial turbine: (a) version 2, with axially-sliding guide vanes; (b) version 1, with radially-offset fixed guide vanes; (c) perspective view of version 2. GV = guide vanes, RB = rotor blades.

3.8. Turbine noise

All turbines operating with air or other gas produce noise. This can be a nuisance if the machine is located near an inhabited area and is not properly shielded, as is the case of many wind turbines. Noise can also be a problem with air turbines for wave energy conversion, especially in shoreline or nearshore applications. Produced noise level increases with machine size and especially with flow velocity and rotor blade speed. This means that it may affect particularly Wells turbines, especially under stalled flow conditions. A noise attenuation chamber had to be retrofitted onto the end of the Wells turbine ducting of the LIMPET shoreline plant (Islay island, Scotland) to reduce the transmitted noise. This turned out to cause mal-distribution of flow during the intake stroke of the turbine; the increased air flow at the bottom of the turbine ducting

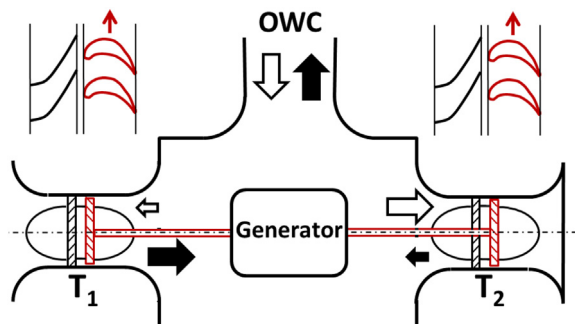


Fig. 39. Twin unidirectional impulse turbine topology.

caused a further increase in stall with an associated reduction in turbine performance [114,115].

Takao et al. [116] performed a model testing investigation on several self-rectifying air turbines and concluded that impulse turbines are superior to Wells turbines on what concerns noise characteristics. An extensive experimental investigation on acoustic characteristics of Wells turbines was carried out at Siegen University, in Germany [13,117]. It was found that, for fixed rotational speed, the sound power radiated by a Wells turbine increases more or less steadily with rising pressure head up to an operating point where the maximum power point is reached. Beyond this point, the turbine stalls and a dramatic increase in sound power is observed. A stalled Wells turbine emits noise that far exceeds all noise levels found in a healthy flow regime.

3.9. Dimensional analysis

Dimensional analysis is widely used in turbomachinery studies (see e.g. Ref. [69]). Its application to air turbines for OWCs is especially useful in two situations: (i) when transposing results from turbine model testing to full-sized prototype; (ii) to study the effects of changes in rotational speed upon the aerodynamic performance curves of a given turbine.

In OWC converters operating under energetic sea conditions, the pressure oscillations in the air chamber may be large enough for changes in air density to be non-negligible. This means that Mach number effects in the turbine flow may be significant. We consider: (i) the same turbine under different working conditions, or (ii) a full-sized turbine and its geometrically similar model. Dimensional analysis requires that three dimensionless quantities take equal values for the similarity relationships to apply: Reynolds number, Mach number and inlet-to-outlet pressure ratio [69]. Not much accurate information is available from the monitoring of full-sized prototype air turbines under real sea conditions. Indeed, most information comes from model testing under laboratory conditions, in most cases with turbine rotor diameters between 0.3 and 0.6 m. Pressure heads achievable in the tests rigs so far used to test self-rectifying air turbines are substantially lower than what can be attained in OWC converters under energetic sea conditions. Consequently, the Mach number equality is usually ignored as a condition for full aerodynamic similarity. At full size, changes in Reynolds number practically do not affect the aerodynamic performance of air turbines [118]. The same is not true if the similarity is to be established between a relatively small model and a large full-sized machine. In any case, Reynolds number effects are ignored or, alternately, accounted for by more or less well established formulae from turbomachinery literature [118]. In what follows, we ignore Mach and Reynolds number effects and assume the air flow through the turbine to be approximately incompressible. Let $p + p_{at}$ (p_{at} = atmospheric pressure) be the instantaneous air pressure in the chamber. Buckingham's theorem yields the

following relationship for the flow through the turbine (see Ref. [118])

$$\Phi = F_\Phi(\Psi), \quad \eta = F_\eta(\Psi), \quad \Pi = F_\Pi(\Psi), \quad (10)$$

where

$$\Psi = \frac{p}{\rho_{at}\Omega^2 D^2}, \quad \Phi = \frac{w}{\rho_{at}\Omega D^3}, \quad \Pi = \frac{P_t}{\rho_{at}\Omega^3 D^5}. \quad (11)$$

Here, w is mass flow rate through the turbine (positive for outward flow), ρ_{at} is atmospheric air density, Ω is the rotational speed (in radians per unit time), D is the turbine rotor diameter and P_t is the turbine power output. In Eqs. (10) and (11), Ψ is dimensionless pressure head, η is aerodynamic efficiency, Φ is dimensionless flow rate and Π is dimensionless aerodynamic torque or dimensionless turbine power output. Functions F_Φ , F_η and F_Π are the same for model and prototype, since these are assumed geometrically similar.

3.10. Turbine performance in random waves

Self-rectifying air turbines in OWCs are subject to oscillations in pressure head and flow rate that, in relative terms, far exceed what is typical of more conventional turbine applications. The flow rate randomly oscillates between negative and positive values with a typical period of 6–12 s. What matters in terms of aerodynamic performance is an average efficiency rather than peak efficiency.

For a given sea state, the probability density function $f_\zeta(\zeta)$ of the surface elevation ζ at a given observation point may be considered Gaussian, an assumption widely adopted in ocean engineering applications. The pressure oscillations $p(t)$ in the air chamber are also random, and may be considered as a Gaussian process within the framework of linear water wave theory (see Section 4) provided that the turbine exhibits a linear pressure-versus-flow-rate characteristic. This is approximately the case of Wells turbines. In such cases, the probability density function $f_p(p)$ of the air pressure oscillations may be written as

$$f_p(p) = \frac{1}{\sqrt{2\pi}\sigma_p} \exp\left(-\frac{p^2}{2\sigma_p^2}\right), \quad (12)$$

where σ_p^2 is the variance, and σ_p is the standard deviation (or root-mean-square) of the pressure oscillation p (see Refs. [12,119]). In dimensionless form (see Section 3.9), the time-averaged value $\overline{\Pi}$ of the turbine power output Π is

$$\overline{\Pi}(\sigma_\Psi) = \frac{1}{\sqrt{2\pi}\sigma_\Psi} \int_{-\infty}^{\infty} \exp\left(-\frac{\Psi^2}{2\sigma_\Psi^2}\right) F_\Pi(\Psi) d\Psi, \quad (13)$$

where

Table 2

Characteristics of Wells turbines of some OWC prototypes. Type: MP = monoplane; BP = biplane; CR = contra-rotating; GV = with guide vanes; VP = variable-pitch; h = hub-to-tip ratio; Z = rotor blade number; c = rotor blade chord; σ = solidity (total bladed area divided by annular area).

Plant	Year	Type	D (m)	h	Z	c (m)	σ	P_t (kW)
Sakata, Japan [109]	1989	MP, GV	1.337	0.75	16	0.1625	0.71	30
Vizhijam, India [110]	1991	MP	2.0	0.6	8	0.380	0.611	150
Islay, UK [111]	1991	BP	1.2	0.62	4 + 4	0.4	0.54	75
OSPREY, UK	1995	CR	3.5					2 × 500
Mighty Whale, Japan [43]	1998	MP, GV	1.7	0.706	8			30
Pico, Portugal [25]	1999	MP, GV	2.3	0.598	8	0.375	0.53	400
LIMPET, UK [26]	2000	CR	2.6	0.62	7 + 7	0.329	2 × 0.34	2 × 250
Pico, Portugal [82,112]	2001	VP	1.7	0.71	15	0.2	0.66	400
Mutriku, Spain [113]	2011	BP	0.75		3 + 3			18



Fig. 40. 2×500 kW contra-rotating Wells turbine of OSPREY, about 1995.

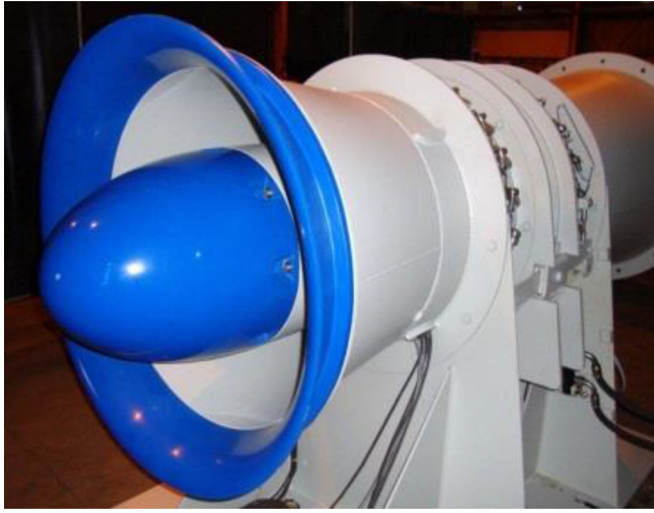


Fig. 41. Axial-flow impulse turbine with controlled-pitch guide vanes, tested in the 1:4th-scale BBDB OWC (the OE Buoy) at Galway Bay, Ireland, in 2011.

$$\sigma_\Psi = \frac{\sigma_p}{\rho_{at} \Omega^2 D^2} \quad (14)$$

is a dimensionless form of σ_p , or, equivalently, is the standard deviation or root-mean-square of the dimensionless pressure head Ψ . An averaged efficiency $\bar{\eta}$ versus σ_Ψ in randomly oscillating air pressure head can be obtained from Eq. (13) (for details, see Refs. [12,119]). These relations, derived for a linear turbine (as is the case of the Wells turbine), can be applied approximately for non-linear self-rectifying turbines (like impulse turbines).

Curves are plotted in Fig. 43 for the instantaneous efficiency η versus dimensionless pressure head Ψ (solid lines) and for the average efficiency $\bar{\eta}$ versus the standard deviation or root-mean-square σ_Ψ (dotted lines). An extensive experimental research program on the aerodynamics of the Wells turbine, involving a large number of geometries, was recently carried out at Universität Siegen, Germany [13,117]. One of the most efficient tested models is

code-named GV6. Its performance curves are plotted in the upper part of Fig. 43, as representative of a highly efficient Wells turbine. The corresponding curves for the biradial turbine were obtained from testing a model [104] and are plotted in the lower part of Fig. 43. Curves of dimensionless averaged power output \bar{P} versus σ_Ψ for the same two turbines can be found in Ref. [79]. The instantaneous peak efficiency is 75% for the Wells turbine and 79% for the biradial turbine. The corresponding maximum values of the average efficiency $\bar{\eta}$ are 67% and 72%, and occur at $\sigma_\Psi \approx 0.022$ and 0.34. Note that the decay of the $\bar{\eta}(\sigma_\Psi)$ curve to the right of its highest point is much more marked for the Wells turbine, which is explained by the sharp drop in efficiency η at a critical value $\Psi \approx 0.072$. In irregular waves, this critical value of Ψ is attained the more frequently the higher the value of σ_Ψ . Assuming the size and rotational speed of the two turbines being such that the maximum values of $\bar{\eta}$ occur for identical values of the standard deviation σ_p of the pressure p , we find, from Eq. (14), for the ratio of the rotor blade tip speeds, $(\Omega D)_{Wells}/(\Omega D)_{birad} = \sqrt{0.33/0.022} \approx 3.9$. This confirms that, for the same applications, the rotor blade tip speed of the Wells turbine is typically much higher than for impulse turbines (and in general other types of air turbines for OWCs).

It is interesting to compare the results plotted in Fig. 43 for the average efficiency $\bar{\eta}$ of air turbines, with typical efficiencies of high-pressure-oil hydraulic PTOs used in oscillating-body WECs. Such information, based on performance of real hydraulic and electrical components and on numerical simulations of the whole WEC, are available in Ref. [120] for a heaving buoy off the coast of Oregon, USA. The PTO efficiency was found to vary widely with sea state, with an annual average of 61% and a maximum value of 72%. It should be noted that the efficiency of hydraulic PTOs substantially vary with the load (and sea state), whereas the aerodynamic efficiency of air turbines (known to be almost independent of Reynolds number) only depends weakly on such factors provided that the rotational speed is appropriately controlled and no constraints on maximum allowed rotational speed are imposed.

3.11. Turbine induced damping

As explained in more detail in Section 4, the hydrodynamic process of energy absorption from the waves by an OWC converter depends on the relationship between the volume flow rate displaced by the OWC motion and the air pressure in the chamber, i.e. the damping provided by the turbine. This is directly related to the volume air flow rate w/ρ through the turbine (positive for outward flow) and the pressure head p available to the turbine (here we assume incompressible air flow with density ρ).

The relationship $w/\rho = f(p)$ depends on the turbine type, geometry, size and rotational speed. It should match the hydrodynamics requirements, which, for a given OWC device, depend on the sea state, especially on the representative wave frequency. For a given turbine geometry (independently of turbine size, rotational speed and air density), the dimensional analysis allows us to write $\Phi = F_\Psi(\Psi)$, where F_Ψ is a functional relationship that characterizes the turbine geometry, Φ is the dimensionless flow rate and Ψ the dimensionless pressure head as defined by Eq. (11).

The Wells turbines are known to be approximately linear turbines, i.e. it is $\Psi = K\Phi$, where K is a factor that depends, among other parameters, on the hub-to-tip diameter ratio and on blade solidity (total bladed area divided by annular area). It follows that

$$\frac{w}{p} = \frac{D}{K\Omega} \quad (15)$$

The hydrodynamics of an OWC converter in a given representative sea state yields a design value $(w/p)_{des}$ for the ratio w/p . If,



Fig. 42. One of the two 250 kW impulse turbines of the bottom-standing OWC plant at Jeju Island, South Korea.

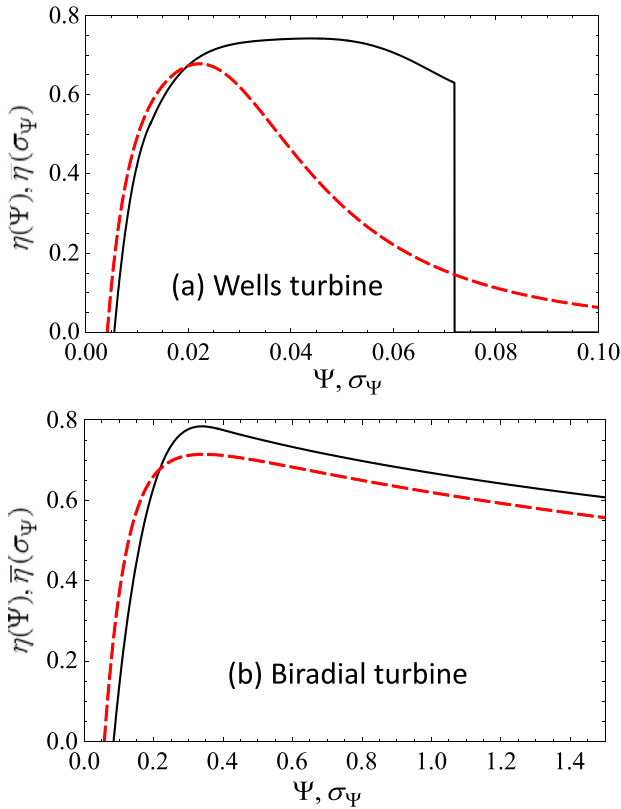


Fig. 43. Dimensionless representation of aerodynamic efficiency η versus pressure head Ψ (solid curves) for the Wells turbine (a) and the biradial turbine (b). The dotted curves represent the average efficiency $\bar{\eta}$ versus the standard deviation σ_Ψ of the pressure in oscillating flow.

besides that, the turbine geometry is specified (i.e. for fixed K), we find a design value $(D/\Omega)_{\text{des}}$ for the ratio D/Ω . A further condition is introduced by the dependence of the turbine efficiency on the dimensionless pressure head $\eta = F_\eta(\Psi)$ (assumed known). Let $\Psi_{\eta_{\max}}$ be the value of Ψ that maximizes the efficiency η . Assuming an “average” or “design” value p_{des} for the pressure head p , we obtain $(\Omega D)_{\text{des}} = p_{\text{des}}^{1/2} \rho^{-1/2} \Psi_{\eta_{\max}}^{-1/2}$. This together with the value $(D/\Omega)_{\text{des}}$, finally gives the design values D_{des} and Ω_{des} . Note that these design

values were optimized for a representative or “design” sea state. The turbine rotational speed should be increased in more energetic states, and decreased in less energetic sea states, if the turbine efficiency is not to be negatively affected. From Eq. (15) we conclude that this changes would imply decreasing, or increasing, the damping ratio w/p , which in turn would affect the efficiency of the hydrodynamic process of wave energy absorption.

The linearity of the Wells turbine makes it different from other turbines. In most other self-rectifying turbines (including those of impulse types), and in conventional axial- and radial-flow water and gas turbines, the pressure head versus flow rate is roughly quadratic, or

$$\frac{w^2}{p} \approx \frac{\rho D^4}{K_1}. \quad (16)$$

This shows that the damping provided by the turbine is approximately independent of the rotational speed. This speed may be adjusted to maximize the turbine efficiency without that affecting the hydrodynamic process.

In real irregular waves and in a wave climate consisting of a wide range of sea states, the turbine optimization procedures are a lot more complex than outlined above. Such procedures are described in Ref. [121] for a fixed-structure OWC and in Ref. [79] for a floating one.

3.12. Concluding remarks

Several types of self-rectifying air turbines were developed since the mid-1970s to equip OWC plants. The axial-flow Wells turbine is the best known. It is also mechanically the simplest turbine, especially the variant without guide vanes, and possibly the cheapest one to construct. The performance characteristics can be adjusted by changing the hub-to-tip diameter ratio and the blade solidity (total bladed area divided by annular area). This can be extended by setting the rotor blades onto two planes (bi-plane turbine). The introduction of guide vanes, as a way of recovering the exit swirl kinetic energy, can improve the peak efficiency by a few percent. A similar effect can be achieved by contra-rotating rotors, but this is a substantially more expensive solution. Multi-stage Wells turbines have been considered for relatively large pressure heads, but this seems never to have been tested. Results from model testing of Wells turbines indicate that peak efficiencies up to about 75% are attainable with the best designs. The basic

conception of the turbine itself, together with limits in the lift-to-drag ratio of aerofoils, makes this value unlikely to be exceeded by more than a few percent. The major limitation of the Wells turbine is the sharp drop in efficiency that occurs whenever the flow rate exceeds the stall-free conditions at the rotor blades. This is particularly damaging in irregular waves, as shown in Fig. 43a. For identical applications and conditions, the rotor blade speed of a (single stage) Wells turbine is much larger than that of any other type of self-rectifying turbine (both the rotor diameter and the rotational speed are larger). While this increases the kinetic energy storage capability by flywheel effect (which may be desirable), it may also have negative effects, namely constraints due to Mach number effects (occurrence of shock waves) and excessive centrifugal stresses.

The main snag about the self-rectifying axial- and radial-flow turbines of impulse type is the presence, under both flow direction conditions, of a row of guide vanes downstream of the rotor. This was found to limit the peak efficiency to about 50%. The use of passively or actively controlled pivoting guide vanes can improve the peak efficiency of such turbines by about 10–15%, but this is achieved at the cost of increased mechanical complexity. An alternative for reducing the aerodynamic losses at the downstream guide vanes is to offset them radially from the rotor. A problem of this configuration is associated with the increased distance the fluid in strongly swirling flow has to travel between the first row of guide vanes and the rotor blades: this is likely to produce significant losses and flow profile distortion due to interaction with the duct wall boundary layers. The only way of totally avoiding this problem is to remove the downstream guide vanes from the flow coming out of the rotor; this is done in the sliding-guide-vane version of the biradial turbine, which allowed a measured peak efficiency of 79% to be attained. Again, this is achieved at the cost of increased mechanical complexity.

Controlling the rotor blade pitch of axial-flow turbines as a way of widening the flow range response has also been attempted, but this introduces even higher mechanical complexity.

Conventional hydraulic and gas turbines of radial- and axial-flow types are very efficient machines, with peak efficiencies in the range of 90–93%. Their use in OWC applications would require a valve mechanism of flow rectification. This has been considered for some multi-OWC floating devices with all (or some) chambers connected to a single turbine through low- and high-pressure ducts.

The power level available to the turbine varies widely with the sea state. Since full-sized air turbines operate at large Reynolds numbers, such variations should not significantly affect the average efficiency of the turbine, provided that its rotational speed is adequately controlled. The same cannot be said of electrical generators, whose efficiency is known to drop substantially at partial loads.

4. OWC modelling

4.1. Theoretical hydrodynamic modelling

Not surprisingly, OWCs were among the first wave energy converters to be theoretically modelled. This was particularly the case of the OWC spar-buoy which was analysed by Michael McCormick, one of the wave energy pioneers, in what were two of the first theoretical papers on wave energy converters to have been published in journal form [45,46]. These were followed, in 1978, by a paper by Evans [6] with analytical solutions for simple geometries: a vertical thin-walled tube-shaped OWC and a two-dimensional one formed by two parallel vertical thin walls. These early papers were based on linear water wave theory, and the inner

free-surface was assumed as a piston-like horizontal flat surface.

A more realistic assumption is a spatially uniform air pressure on the, in general warped, interior free surface. This model was adopted for the first time in Ref. [122], where a two-dimensional OWC was theoretically analysed. The uniform surface pressure model was generalized in Ref. [123] to arbitrary geometries. The adoption of the rigid piston model was (and is) a way of taking advantage of the theory developed prior to the mid-1970s of the interaction between waves and floating bodies, especially ships (see e.g. Refs. [124,125]). This theory was later extended in Ref. [126] to oscillating-body wave energy converters (see also [127]). The concepts of body velocity and force in oscillating-body theory are replaced by air flow rate and air pressure in the uniform free-surface pressure approach to OWC modelling.

Assuming linear water wave theory to apply, the governing equation for the rigid piston model of a fixed-structure OWC (Fig. 44a) may be written as

$$m \frac{d^2x}{dt^2} = -\rho g Sx + f_r + f_e - Sp. \quad (17)$$

Here, x is a vertical coordinate defining the piston position (with x increasing upwards and $x = 0$ in the absence of incident waves), m is the mass of the piston (possibly equal to zero), S is the piston area, ρ is water density, g is acceleration of gravity, f_r is the hydrodynamic radiation force on the piston due to the piston motion in otherwise calm water, f_e is the excitation force on the assumedly fixed piston due to the incident wave field, and p is the excess pressure of air in the chamber ($p = 0$ in the absence of waves or if the chamber is fully open to the atmosphere). We may write $Sx = V_0 - V$, where $V(t)$ is the instantaneous volume of air in the chamber and V_0 is its value in the absence of waves.

If the uniform pressure distribution on the inner free-surface is the adopted model (Fig. 44b), we introduce the volume flow rate $q(t)$ displaced by the motion of the internal free-surface ($q > 0$ for upward motion). It is $q = -dV/dt$. The linearization allows us to decompose

$$q(t) = q_r(t) + q_e(t). \quad (18)$$

Here q_r is the radiation flow rate due to the oscillating pressure p in the chamber in the absence of incident waves, and q_e is the excitation flow rate due to the incident wave field if $p = 0$.

In both models, the air pressure $p(t)$ is related to the instantaneous volume $V(t)$ of air in the chamber and its time history, to the aerodynamic characteristics of the turbine, and to the thermodynamics of the air compression/decompression process that takes place in the chamber. We assume first that a linear relationship applies between, on the one hand, the piston velocity dx/dt or the displaced volume-flow rate q , and, on the other hand, the pressure oscillation p . This assumption is taken as in linear system theory where the response to a sinusoidally time-varying signal is another sinusoidally time-varying signal, possibly with a phase difference between both. Under such conditions, the whole (wave-to-pneumatic) system is linear. If in addition the incident waves are regular of radian frequency ω , we may employ a frequency domain analysis and write

$$\{x, f_r, f_e, q, q_r, q_e, p\} = \{X, F_r, F_e, Q, Q_r, Q_e, P\}e^{i\omega t}, \quad (19)$$

where X, F_r, F_e, Q, Q_r, Q_e and P are, in general complex, amplitudes. Here, and wherever a physical quantity is equated to a complex expression, it should be understood that the real part is to be taken. Note that the amplitude ratios $P/(i\omega SX) = \alpha - i\beta$ and $P/Q = \alpha - i\beta$, (α, β real), involving the chamber pressure and the air flow rate displaced by the piston motion or the inner free-surface motion, may

be complex due to the air compressibility effect in the chamber. This introduces a phase difference between the flow rate q and the flow rate through the air turbine (see Section 4.2).

As is usual in the frequency domain analysis, we further write, for the radiation force on the piston, $F_r = (\omega^2 A - i\omega B)X$. Here A (added mass) and B (radiation damping coefficient) are real, and B cannot be negative (see Refs. [123,127]). Correspondingly, we write, for the radiation flow rate, $Q_r = -(G + iH)P$ (G and H are real) where G is the radiation conductance and H is the radiation susceptance (see Ref. [127]). The four radiation coefficients A , B , G and H depend on wave frequency ω . From Eq. (17), we easily obtain, for the piston model,

$$X \left[-\omega^2(m + A) + i\omega B + \rho g S \right] = F_e - SP \quad (20)$$

or

$$X \left[-\omega^2(m + A) + i\omega(B + S^2\alpha) + \rho g S + S^2\omega\beta \right] = F_e. \quad (21)$$

From Eq. (18), we find, for the uniform surface pressure distribution model,

$$P \left(\frac{1}{\alpha - i\beta} + G + iH \right) = Q_e. \quad (22)$$

These are the equations to be solved in the frequency domain.

It may be of interest to relate the added mass A and the radiation damping coefficient B to the radiation conductance G and the radiation susceptance H . To do that, we consider the piston model, and assume no incident waves. Consequently, in Eq. (17), we set $F_e = 0$ and replace X by X_r (complex amplitude of the piston displacement due to the time varying air pressure only). The complex amplitude of the flow rate displaced by the piston motion is $i\omega S X_r$ which, as for Q_r , we decompose as $i\omega S X_r = -(G_1 + iH_1)P$, where subscript 1 is used to denote that the radiation conductance G_1 and the radiation susceptance H_1 are defined for the piston model, and so are not expected to be exactly equal to G and H . Then we are left with

$$\frac{-(G_1 + iH_1)P}{i\omega S} \left[-\omega^2(m + A) + i\omega B + \rho g S \right] = -SP \quad (23)$$

or

$$\frac{S^2 G_1}{G_1^2 + H_1^2} = B, \quad (24)$$

$$\frac{\omega S^2 H_1}{G_1^2 + H_1^2} = -\omega^2(m + A) + \rho g S. \quad (25)$$

Equations (24) and (25) relate the pair of hydrodynamic coefficients (G_1, H_1) to the pair (A, B) . We recall that the pairs of hydrodynamic coefficients (G_1, H_1) and (G, H) are physically similar, but their numerical values do not coincide because the two models are not expected to yield exactly equal results.

By setting $P = 0$ in Eq. (20), we easily find the following relationship between the complex excitation force amplitude F_e and the complex excitation flow rate amplitude $Q_{e,1}$, where, as above, the subscript 1 indicates that $Q_{e,1}$ is not exactly equal to Q_e ,

$$Q_{e,1} = i\omega S \left[-\omega^2(m + A) + i\omega B + \rho g S \right]^{-1} F_e. \quad (26)$$

In general, the piston velocity dx/dt and the displaced volume-flow rate q are not proportional to the pressure oscillation p . The nonlinearities may be introduced by the air chamber thermodynamics or by the aerodynamic performance curves of the turbine. In such cases, the frequency domain analysis is no longer applicable and has to be replaced by a time domain analysis. In particular, the expression of the radiation force on the piston involves a convolution integral, as in the so-called Cummins equation in ship hydrodynamics [128], extended to oscillating-body wave energy converters in Ref. [129]. Similarly, the radiation flow rate q_r can be expressed by a convolution integral as done in Ref. [130]

$$q_r(t) = - \int_{-\infty}^t h_r(t - \tau) p_c(\tau) d\tau. \quad (27)$$

The memory function h_r is related to the radiation susceptance G through the Fourier transform

$$h_r(s) = \frac{2}{\pi} \int_0^\infty G(\omega) \cos \omega s d\omega. \quad (28)$$

The surface pressure distribution model was extended from fixed structure to floating structure OWCs in Ref. [131]. The theoretical modelling of OWCs based on the free-surface uniform pressure model is the subject of a full chapter in Falnes' book [127].

Analytical solutions based on the surface pressure distribution model were obtained for several simple geometries by integrating Laplace's equation for the velocity potential function by the method of separation of variables together with the matched eigenfunction expansion method. This is the case of a two-dimensional OWC with vertical thin walls [132], a vertical thin-walled circular cylindrical OWC [133] and a circular cylindrical OWC at the tip of a breakwater [134] or the tip of a coastal corner [135]. More complex geometries include a floating vertical axisymmetric OWC [136] and a two-dimensional dual-chamber OWC on stepped bottom [137]. For

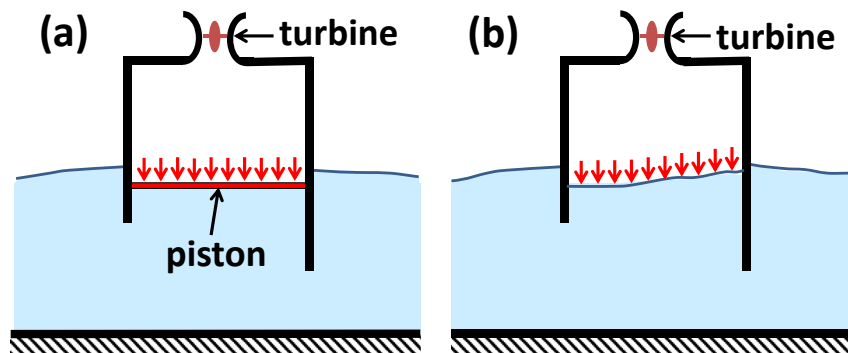


Fig. 44. Schematic representation of OWC modelling: (a) piston model; (b) free-surface uniform pressure model.

non-diffracting OWC structures, analytical solutions can be derived from the expressions for the wave field induced by time-harmonic surface pressure distributions [124]. This was the method adopted in Ref. [138] for an infinite linear array of OWCs, which was extended to other array configurations in Ref. [139].

Even if linear water wave theory is assumed to apply (which implies irrotational flow and small amplitudes for the outer and inner free-surface motions), complex geometries require the application of numerical methods. These are usually based on the computation of hydrodynamic coefficients as defined above. Commercial codes based on the boundary element method (BEM) are available to compute such coefficients for ships and marine structures. Such codes, like WAMIT, ANSYS/Aqwa and Aquaplus, have also been frequently employed by the wave energy conversion community. Their use assumes an oscillating body or a set of oscillating bodies in a wave field to be an acceptable approximation. In the case of OWCs, this implies the inner free-surface to be simulated by a rigid piston. The possibility of employing commercial codes based on the BEM is possibly the main reason why the rigid piston model, rather than the more realistic surface pressure distribution approach, is so popular in OWC theoretical/numerical modelling. It is possible to modify a BEM code developed for the study of floating bodies and extend it to the modelling of OWCs. This was done with the radiation-diffraction code Aquadyn developed at Ecole Centrale de Nantes, France, by modifying the dynamic boundary condition on the internal water free surface to account for the imposed oscillatory uniform pressure distribution within the chamber [140]. The modified code was used to model the shoreline OWC plant constructed at the island of Pico, Azores, including the effect of surrounding coastline and non-flat bottom [141]. A method was developed in Ref. [142] to apply a three-dimensional BEM like WAMIT to model an OWC device accounting for the appropriate interior free-surface boundary condition.

The methods mentioned above are based on Laplace's equation and linear water wave theory, and are unable to model non-small wave and body-motion amplitudes and real fluid dissipative effects like viscous friction, turbulence and eddy shedding. Such effects may be important especially in the more energetic sea states and under conditions close to resonance. Computational fluid dynamics (CFD) methods may be employed to account for such effects. They are usually based on the numerical integration of the Reynolds-averaged Navier–Stokes (RANS) equations together with an appropriate turbulence model. Commercial and open-source codes are available and have been used for wave energy conversion applications, including especially OWCs. In some cases, the computational domain has included the air flow field in the OWC chamber. The use of such codes implies heavy computing. In some (possibly most) cases (see e.g. Refs. [143–148]), the geometry is two-dimensional (the so-called numerical wave tank) and the waves are regular (the computational effort required for calculations in irregular waves to be of statistical value can be prohibitive).

4.2. Thermodynamics of air chamber

The volume of the air chamber of the OWC converter should be large enough to avoid ingestion of water by the air turbine under rough sea conditions. Typical design values of the air chamber volume divided by the area of the OWC free surface range between 3 and 8 m, and are affected by tidal oscillations in fixed-structure OWC devices. An increase in this ratio is not necessarily detrimental to the efficiency of the energy conversion. Obviously, if the volume increases to very large values, the amplitude of the air pressure oscillations becomes very small, and the capability of the device to absorb wave energy vanishes. The spring-like effect of air compressibility in the chamber increases with chamber volume,

and is important in a full-sized OWC converter. This effect was modelled for the first time in Ref. [149], and shortly afterwards in Ref. [150]. In both papers, and in many subsequent ones (see e.g. Ref. [151]), a simple isentropic relationship between air pressure and density was assumed. In fact, the aerodynamic and thermodynamic processes that take place in the air chamber and turbine of an OWC converter are quite complex; they were analysed in detail in Ref. [152]. It seems reasonable to assume that they are approximately adiabatic. Indeed, the temperature oscillations in the air chamber are relatively small and their time scales (a few seconds) are too short for significant heat exchanges to occur across the chamber walls and across the air–water interface, in comparison with the energy flux in the turbine.

However, even if the process is assumed as adiabatic, significant changes in specific entropy occur in the flow through the turbine, due to viscous losses. Such changes can be related to turbine efficiency. We recall that the pressure in the chamber is $p_{at} + p$, where p_{at} is the atmospheric pressure. During inhalation, it is $p < 0$, and air with specific entropy $s > s_{at}$ is admitted to the chamber, where a highly turbulent mixing process takes place (the increase in specific entropy in the flow through the turbine is due to real fluid effects). During exhalation, $p > 0$, air leaves the chamber through the turbine in a process at approximately constant specific entropy for the air remaining in the chamber. The inhalation and exhalation processes in an OWC were studied in some detail in Ref. [152]. A polytropic relationship between the pressure $p + p_{at}$ and the density ρ_{ch} in the air chamber was proposed in Ref. [118]

$$\frac{p_{at} + p}{\rho_{ch}^k} = \frac{p_{at}}{\rho_{at}^k}, \quad (29)$$

where k is the polytropic exponent that is related to the average efficiency $\bar{\eta}$ of the turbine (see Section 3.10 and [118] for a definition of average efficiency). A good approximation to the relationship proposed in Ref. [118] is

$$k = 0.13\bar{\eta}^2 + 0.27\bar{\eta} + 1. \quad (30)$$

If $\bar{\eta} = 1$ (perfectly efficient turbine), then $k = 1.4$, and Eq. (29) becomes simply the isentropic pressure–density relationship. If $\bar{\eta} = 0$, it is $k = 1$ and Eq. (29) becomes the isothermal relationship.

4.3. Model testing of OWCs

The theoretical modelling based on linear water wave theory is an essential step in the development of wave energy converters. It provides insights and important information at relatively low costs, in general in a relatively fast way. However, there are important non-linear effects that are not accounted for by this kind of modelling, namely those associated with large amplitude waves, large amplitude motions of the wave energy converter or oscillating-water-column, and real fluid effects due to viscosity, turbulence, and vortex shedding. Commercially available computational-fluid-dynamics (CFD) codes, usually based on the numerical integration of the Reynolds-averaged Navier–Stokes (RANS) equations, may be used to account for such effects. However, even such codes, apart from being computationally demanding, require some experimental validation. Therefore physical model testing in a wave flume or wave tank is normally the next step. The scales range between about 1:100th in small wave flumes to about 1:10th in the largest wave tanks. Tests at larger scales (typically 1:4th to 1:3rd scale) sometimes take place in sheltered sea locations. We may apply dimensional analysis techniques to relate the conditions in model testing to those of the full-sized prototype in real sea conditions. Dimensional analysis in

model testing of wave energy converters in general is addressed in the pioneer book by McCormick [47] and more recently in Refs. [153–155]. The testing of OWCs raises specific issues, related to the turbine and the air compressibility effect in the chamber, that are addressed in Refs. [118,156].

When performing model testing in waves, it is assumed that the wetted part of the model is an exact geometric representation of the full-scale prototype. This geometric similarity is supposed to apply also to the bottom and surrounding walls. The incident waves may be represented by a given variance density spectrum (Pierson–Moskowitz or other (see e.g. Ref. [157]), $S_f(H_s, T_e; f)$, where H_s is the significant wave height, T_e is energy period (or some other representative period) and f is frequency. In the case of regular waves, H_s and T_e are simply the wave height and period.

Let L be a characteristic length (this could be a diameter in the case of an axisymmetric device). As before, we denote by $p + p_{\text{at}}$ the pressure in the air chamber of the OWC converter. Buckingham's theorem of dimensional analysis allows us to write

$$\Pi_1 = \Theta(H_s/L, \text{Fr}, \text{Re}, \Pi_p). \quad (31)$$

Here, Θ is a function, $\text{Fr} = L^{1/2}g^{-1/2}T_e^{-1}$ is a Froude number, $\text{Re} = L^2\nu^{-1}T_e^{-1}$ is a Reynolds number, $\Pi_p = pL^{-1}\rho^{-1}g^{-1}$ is dimensionless pressure, $\Pi_1 = PL^{-7/2}\rho^{-1}g^{-3/2}$ is dimensionless power, and ρ and ν are water density and kinematic viscosity respectively. Identical relationships could be established by replacing Π_1 by other dimensionless quantities. If the four dimensionless variables $\text{Fr}, \text{Re}, H_s/L$ and Π_p take equal values in the model and the full-sized prototype, the same will be true for Π_1, Π_2, \dots

Let the subscripts m and F denote the model and the full-sized prototype. The length scale is defined as $\varepsilon = L_m/L_F$. The constancy of the Froude number Fr and the Reynolds number Re cannot be satisfied simultaneously, since this would require $\nu_m/\nu_F = \varepsilon^{3/2}$, a condition that is obviously unachievable in practice if ε is not close to unity. In model testing, the effects due to variations in Froude number are almost always much more important than those associated with changes in Reynolds number, and so the Reynolds number is ignored as a modelling rule.

The expression of dimensionless power $\Pi_1 = PL^{-7/2}\rho^{-1}g^{-3/2}$ shows that the scale ratio for power is $\varepsilon^{7/2}$ (if variations in water density ρ are neglected). In model testing of wave energy converters in the largest wave tanks, the length scale ε in general does not exceed about 1:10th. This implies a maximum power ratio of about 1:3200. In the case of an OWC wave energy converter, this scale is too small for the turbine to be simulated adequately by a mini-turbine. The usual procedure is to simulate the turbine by an orifice, if the turbine is of impulse type or by a layer of porous material, where the flow is approximately laminar and simulates a linear turbine like the Wells turbine. Only in tests performed under real sea conditions at scales not less than about 1:4th, is a real turbine fitted to the model. This was done in the sheltered waters of Galway Bay, Ireland, at scale 1:4th, with a Backward Bent Duct Buoy (BBDB) (the OE Buoy) fitted first with a Wells turbine and later with an impulse turbine [41,42], Fig. 18.

We consider now that the Froude geometric similarity is extended to the part of the device located above water level, namely the air chamber and its air volume V , i.e. $V_m/V_F = \varepsilon^3$. This would allow realistic representation of water motion inside the chamber and provide information on how to avoid green water from reaching the air turbine. However, that would require $p_{\text{at},m}/p_{\text{at},F} = \varepsilon \delta$. ($\delta = \rho_m/\rho_F$) (see Ref. [118]) The latter condition, concerning atmospheric pressure, is obviously impossible to satisfy in practice if the length scale ε is not close to unity. This impossibility was recognized in Ref. [156] and examined in more detail in Ref. [118].

Now we assume more realistically that the atmospheric pressure is the same at both scales $p_{\text{at},m} = p_{\text{at},F}$. We further assume that the pressure oscillation p is much smaller than the atmospheric pressure, which would exclude the more energetic sea states at full scale. The following similarity condition can be obtained for the air chamber volume ratio [118]

$$\frac{V_m}{V_F} = \frac{k_m}{k_F} \varepsilon^2 \delta^{-1}, \quad (32)$$

where k is the polytropic exponent as defined in Section 4.2. In model testing at large scale (say about 1:4th to 1:3rd) performed in the sea, it is $\delta = 1$ (equal water density). If in addition an appropriately scaled-sized turbine is used to realistically simulate the full-sized machine, it is $k_m \equiv k_F$ (if the turbine model is not too small). Then, from Eq. (32), we have

$$\frac{V_m}{V_F} = \varepsilon^2. \quad (33)$$

A result identical to Eq. (32) was first obtained in Ref. [149], based on a frequency-domain analysis of the hydrodynamics and a linearized isentropic assumption. It later appeared in other papers (e.g. Refs. [150,151,155–158]). It shows that the scale ratio for air chamber volume should be ε^2 , rather than ε^3 . Failure to meet this condition may result in substantial errors in the conversion to full scale of the experimental data at a smaller scale (for a numerical case study, see Ref. [118]).

If the OWC device is of fixed structure (possibly bottom-standing), it is not difficult to satisfy condition (32) at small model scale. One simple way of achieving that is to connect the air chamber of the model to a rigid-walled reservoir of air of appropriate volume. This procedure was adopted in the model testing of the bottom-standing OWC installed in 1999 on the island of Pico, Azores, Portugal, as reported in Ref. [158]. If however a floating OWC device is to be modelled at small scale, this could introduce difficulties because the reservoir is likely not to be small compared with the device's size, and possibly is a lot larger.

If the model scale is large enough (say not less than about 1:4th), the model may be equipped with a real turbine (rather than a simple orifice or a porous plug). In such cases (in which the water density is that of sea water), if the model turbine is geometrically similar to the full-sized one and both are equally efficient, the following similarity conditions can be obtained for the rotor diameter D and rotational speed Ω (see Ref. [118])

$$\frac{D_m}{D_F} = \varepsilon, \quad \frac{\Omega_m}{\Omega_F} = \varepsilon^{-1/2}. \quad (34)$$

This shows that the linear scale for the turbine should be the same as for the wetted part of the structure.

5. Control

5.1. Reactive phase control

In WECs of oscillating-body and OWC types, the highest efficiency of wave energy absorption from regular waves is attained under conditions close to resonance. Especially in the case of relatively small devices (the so-called point absorbers), it is well known that the resonance bandwidth is relatively narrow, which implies that their performance in irregular waves is relatively poor. Besides, for many point absorbers, the natural frequency of resonance is higher than the typical frequency of the waves. Phase control has been proposed to improve these situations [159–161]. Reactive phase control is a way of doing that: reactive power

contributes nothing to the average delivered power and is back-and-forth exchange of energy between the PTO and the oscillating system. This energy may be stored in a flywheel, a gas accumulator, a battery of condensers, or may be supplied by the electrical grid. A major drawback of reactive phase control is the energy loss by dissipative processes inherent to the back-and-forth energy exchange, especially if the magnitude of such exchanged energy is comparable to, or even significantly larger than, the net absorbed energy. This may be the case of point absorbers. Reactive phase control is particularly appropriate if the PTO is a high-pressure hydraulic circuit with gas accumulator, where the fluid flow may be reversed by controlling the valve system. This may also be achieved in the case of direct electrical energy conversion (linear or rotating generator) by two-way exchange of energy with the grid.

Reactive control has also been considered for OWCs equipped with self-rectifying air turbines. If the setting angle of the rotor blades of a Wells turbine is controllable within a sufficiently wide range (say $\pm 20^\circ$), then the machine can operate either as a turbine or as a compressor, and may be used to achieve reactive control [162–164]. A 400 kW variable-pitch Wells turbine, whose sophisticated control mechanism was driven by eddy currents (Fig. 29), was built to be tested in the Pico plant, Azores, Portugal [82,112], but was never installed. The relatively modest efficiency of the Wells turbine, especially when operating in the compressor mode, severely limits the gains from reactive control [165]. This, in addition to the much higher mechanical complexity of the turbine and inherent reliability problems, has deterred the use of reactive control in OWCs.

5.2. Phase control by latching

An alternative to reactive phase control is control by latching. This was first proposed for single oscillating bodies reacting against a fixed reference frame (in general the sea bottom) [160], and consists in latching the body in a fixed position during certain intervals of the oscillation cycle.

In principle, reactive control may be optimal, i.e. may allow the theoretical maximum wave energy capture, as predicted by linear water wave theory, to be achieved in unconstrained amplitude conditions (such optimal control is non-causal). This is not the case of control by latching, that is necessarily suboptimal [127]. On the other hand, latching control avoids the two-way energy transfer and the associated energy dissipation that characterize a reactively phase-controlled PTO. In the case of an OWC converter, latching is achieved by closing a valve in series with the turbine.

Latching control of an OWC was analysed for the first time in Ref. [166], where air compressibility was ignored, and [150] where the air compressibility in the chamber was accounted for, but only regular waves were considered and the analysis was in the frequency domain. Both papers considered a fixed-structure OWC. Pontryagin maximum principle was used in Ref. [166] to show that the optimal control is bang–bang, i.e. the position of the valve is either fully open or fully closed.

There are specific problems related to latching control of an OWC. One is the compressibility of the air in the chamber that acts as a spring and prevents the water column to remain fixed with respect to the structure, even if the air flow is stopped at the entrance to the turbine. Besides, it should be noted that such compressibility may remove the constraint of the latching threshold having to coincide with an instant of zero (relative) velocity. Another problem, especially if the turbine is of axial-flow type (as the Wells turbine and most self-rectifying impulse turbines), is the practical difficulty of designing and constructing a valve with a response time not exceeding a few tens of a second. A

very fast and mechanically very complex valve with an elastomeric membrane was designed and constructed to be mounted in series with the 400 kW variable-pitch Wells turbine at the Pico, Azores OWC plant [167], but was never installed. Latching may be less difficult if the turbine is of radial-flow type, in which case an axially-sliding cylindrical valve with a relatively small stroke may be positioned close to the rotor [168].

The forces involved in latching of oscillating-body WECs may be very large, and have to be supported by the PTO or by a special braking system. This has been regarded as a major problem for this type of phase control. Latching forces on air valves are much smaller in the case of OWCs, since the area of the valve surface subject to the chamber pressure is a small fraction of the area of the water column free surface.

Model testing of a fixed-structure OWC showed that substantial gains can be achieved by latching based on a causal algorithm [169] (air compressibility effects were not simulated). As in the case of an oscillating two-body WEC versus a single-body one, latching control of a floating OWC converter raises more difficult problems than for a fixed-structure OWC, since the closure of the latching valve does not stop the motion either of the OWC or of the floater. Numerical simulations of latching control of an OWC spar-buoy in regular waves revealed that large gains in produced energy can be achieved over a wide range of wave frequencies [170]. However the gains were found to be more modest when similar methods, namely causal control, were extended to irregular waves [171], which seems to indicate that more sophisticated control methods, possibly model predictive control, will be required for more satisfactory results. Latching control of OWCs appears as a way of substantially increasing the power produced by OWCs that is worth further investigation.

5.3. Turbine rotational speed and air flow control

The rotational speed should be adjusted to the pneumatic energy level available to the turbine, more precisely to the standard deviation (or root-mean-square) σ_p of the pressure oscillation p . In Section 3.10, it was shown from dimensional analysis that the average efficiency $\bar{\eta}$ of a given turbine (or a set of geometrically similar turbines) is a function of the dimensionless standard deviation (or root-mean-square) σ_Ψ of the pressure oscillation p . In particular, its maximum value $\bar{\eta}_{\max}$ occurs for $\sigma_{\Psi,\max}$, the corresponding value for the averaged turbine power output being \bar{P}_{\max} . In the case of the Wells turbine and the biradial turbine considered in Section 3.10, it is $\sigma_{\Psi,\max} = 0.022$ and 0.34 , respectively. From the definition of σ_Ψ (Eq. (14)), it follows that the rotational speed Ω should be proportional to $\sqrt{\sigma_p}$. Apart from affecting the turbine aerodynamic efficiency, changes in rotational speed also affect the damping provided by the PTO (i.e. the relationship between pressure and flow rate) and in this way affect the hydrodynamic performance of the wave energy absorption process. For this reason, the control algorithm for the rotational speed should take into account both the hydrodynamic and the aerodynamic efficiencies. An algorithm that has been proposed based, on numerical simulation of fixed structure and floating OWCs, is of the form

$$T_{\text{em}} = \text{constant} \times \Omega^\zeta, \quad (35)$$

where T_{em} is the instantaneous electromagnetic torque on the generator rotor, Ω is the instantaneous rotational velocity and ζ is an exponent taking a value typically not very different from 2, depending on the OWC and turbine (see Refs. [79,119,172]). This algorithm should be implemented in the programmable logic controller (PLC) of the plant through the power electronics. Note that it should be exactly $\zeta = 2$ if the average aerodynamic efficiency

of the turbine rather than the overall average efficiency is to be maximized. The implications of rotational speed control on the electrical equipment are addressed in Ref. [173].

Control algorithm (35) may yield values for the rotational speed that, in the more energetic sea states, exceed what should be allowed from the viewpoint of centrifugal stresses. This is especially critical in the case of Wells turbines, because of their typically high rotor blade tip speed; a maximum limit about 150–170 m/s has sometimes been established for the blade tip speed. Such constraint results, in the case of the more energetic sea states, in the value of σ_ψ substantially exceeding $\sigma_{\psi,\max}$ as defined above. Fig. 43a shows that the Wells turbine average efficiency $\bar{\eta}$ decays rapidly with σ_ψ for $\sigma_\psi > \sigma_{\psi,\max}$. To prevent such unwanted efficiency decay to low values in the more energetic sea states, it has been proposed to install an air valve in plants equipped with a Wells air turbine. The valve is either in parallel with the turbine (relief valve) to limit the magnitude the pressure head p [172,174], or in series with the turbine to limit the flow rate [130]. This kind of strategy was recently implemented at the Pico OWC plant, taking advantage of the plant being equipped with a relief valve. The chamber hydrodynamics are forecasted using a neural network that considers wave measurements made 60 m up wave and other operational, environmental and preceding wave parameters [175].

6. Conclusions

The OWC was the first concept for wave energy conversion to be developed, and is still the favourite technology among a large part of the wave energy conversion community. It can be employed in isolated shoreline or nearshore situations, integrated into a breakwater, or in single- and multi-OWC floating plants. From the mechanical viewpoint, the PTO is particularly simple and reliable: the only moving part is the rotor of an air turbine, located above sea water, directly driving a conventional electrical generator.

The overall efficiency of the wave-to-wire energy conversion chain is critically dependent on the performance of the air turbine. Substantial improvements were achieved in this respect since the early self-rectifying air turbines were proposed in the mid-1970s: the axial-flow Wells and impulse turbines. Model testing shows that peak efficiencies close to 80% and average efficiency in random waves above 70% can be attained by new-generation turbines. This places the air-turbine PTO in close competition with the high-pressure hydraulic circuit or the direct electrical energy conversion by linear generator. It seems not unreasonable to expect that efficiencies closer to what is typical of more conventional turbines – hydraulic, steam and gas turbines – will be attained in the near future.

Theoretical hydrodynamic modelling of OWCs based on linear water wave theory and hydrodynamic coefficients is still the most frequently adopted approach, especially if that involves control studies. CFD computational tools, based on the Reynolds-averaged Navier–Stokes (RANS) equations are being increasingly employed, although in many cases restricted to two-dimensional geometries and regular waves.

Like for wave energy converters in general, an essential step in the development of OWCs is model testing, usually in wave tank or wave flume. The air compressibility effect in the air chamber and the simulation of the air turbine raise special problems in model testing that in many cases failed to be adequately addressed.

Phase control is an area from which substantial improvements in power efficiency, and hence economic viability, can be expected at relatively little extra costs. In the case of OWCs, phase control by latching appears as the most promising approach, although theoretical control problems are still to be appropriately solved before practical implementation.

Changes in rotational speed affect the aerodynamic efficiency of

the turbine and, in general to a lesser extent, the hydrodynamic efficiency of the wave absorption process. Algorithms have been proposed to control the rotational speed, expressing the electromagnetic torque on the generator rotor as a function of the instantaneous rotational speed.

Acknowledgements

This work was funded by the Portuguese Foundation for the Science and Technology (FCT) through IDMEC, under LAETA, project UID/EMS/50022/2013. The second author was supported by FCT researcher grant No. IF/01457/2014.

References

- [1] S. Barstow, G. Mork, D. Mollison, J. Cruz, The wave energy resource, in: J. Cruz (Ed.), *Ocean Wave Energy*, Springer, Berlin, 2008, pp. 93–132.
- [2] J. Falnes, A review of wave-energy extraction, *Mar. Struct.* 20 (2007) 185–201.
- [3] B. Drew, A.R. Plummer, M. Sahinkaya, A review of wave energy converter technology, *Proc. Inst. Mech. Eng. Part A: J. Power Energy* 223 (2009) 887–902.
- [4] A.F. de O. Falcão, Wave energy utilization: a review of the technologies, *Renew. Sustain. Energy Rev.* 14 (2010) 899–918.
- [5] I. López, J. Andreu, S. Ceballos, I. Martínez de Alegria, I. Kortabarria, Review of wave energy technologies and the necessary power-equipment, *Renew. Sust. Energy Rev.* 27 (2013) 413–434.
- [6] D.V. Evans, The oscillating water column wave-energy device, *J. Inst. Math. Appl.* 22 (1978) 423–433.
- [7] Carbon Trust, Oscillating Water Column Wave Energy Converter Evaluation Report, 2005. Available at: <http://www.carbontrust.com/media/173555/owc-report.pdf> (accessed 7.03.15.).
- [8] T.V. Heath, A review of oscillating water column, *Philos. Trans. R. Soc. A* 370 (2012) 235–245.
- [9] T. Setoguchi, S. Santhakumar, H. Maeda, M. Takao, K. Kaneko, A review of impulse turbines for wave energy conversion, *Renew. Energy* 23 (2001) 261–292.
- [10] T. Setoguchi, M. Takao, Current status of self rectifying air turbines for wave energy conversion, *Energy Conv. Manag.* 47 (2006) 2382–2396.
- [11] R. Curran, M. Folley, Air turbine design for OWCs, in: J. Cruz (Ed.), *Ocean Wave Energy*, Springer, Berlin, 2008, pp. 189–219.
- [12] A.F.O. Falcão, L.M.C. Gato, Air turbines, in: A.A. Sayigh (Ed.), *Comprehensive Renewable Energy* vol. 8, *Ocean Energy*, Elsevier, Oxford, 2012, pp. 111–149.
- [13] R. Starzmann, *Aero-acoustic Analysis of Wells Turbines for Ocean Wave Energy Conversion* (Doctoral thesis), Universität Siegen, Germany, 2012. Fortschr-Ber VDI Reihe 7, Nr 500, Düsseldorf: VDI Verlag.
- [14] D. Ross, *Power from the Waves*, Oxford University Press, Oxford, 1995.
- [15] Y. Masuda, Wave-activated generator, in: Int. Colloq Exposition Oceans, Bordeaux, France, 1971.
- [16] Y. Masuda, An experience of wave power generator through tests and improvement, in: A.F. de O. Falcão, D.V. Evans (Eds.), *Hydrodynamics of Ocean Wave-energy Utilization*, Springer, Berlin, 1986, pp. 445–452.
- [17] Y. Masuda, M.E. McCormick, Experiences in pneumatic wave energy conversion in Japan, in: M.E. McCormick, Y.C. Kim (Eds.), *Utilization of Ocean Waves – Wave to Energy Conversion*, Amer Soc Civil Eng, New York, 1986, pp. 1–33.
- [18] H. Hotta, T. Miyazaki, S.I. Ishii, On the performance of the wave power device Kaimei, in: Proc 7th Int Conf Offshore Mech Arct Eng, New York, 1988, pp. 91–96.
- [19] C. Grove-Palmer, Wave energy in the United Kingdom – A review of the programme June 1975–March 1982, in: H. Berge (Ed.), Proc 2nd Int Symp Wave Energy Utilization, Trondheim, Norway, 1982, pp. 23–54.
- [20] T.J.T. Whittaker, S.J. McIlwaine, S. Raghunathan, A review of the Islay shoreline wave power station, in: Proc First European Wave Energy Symp, Edinburgh, 1993, pp. 283–286.
- [21] H. Ohneda, S. Igarashi, O. Shinbo, S. Sekihara, K. Suzuki, H. Kubota, et al., Construction procedure of a wave power extracting caisson breakwater, in: Proc 3rd Symp Ocean Energy Utilization, Tokyo, 1991, pp. 171–179.
- [22] M. Suzuki, C. Arakawa, S. Takahashi, Performance of a wave power generating system installed in breakwater at Sakata port in Japan, in: Proc 14th Int Offshore Polar Eng Conf, Toulon, France, 2004.
- [23] M. Ravindran, P.M. Koola, Energy from sea waves – the Indian wave energy program, *Curr. Sci.* 60 (1991) 676–680.
- [24] K. Mala, S.N. Badrinath, S. Chidanand, G. Kailash, V. Jayashankar, Analysis of power modules in the Indian wave energy plant, in: Proc Annual IEEE India Conf INDICON, 2009, pp. 95–98.
- [25] A.F. de O. Falcão, The shoreline OWC wave power plant at the Azores, in: Proc 4th European Wave Energy Conf, Aalborg, Denmark, 2000, pp. 42–47.
- [26] T. Heath, T.J.T. Whittaker, C.B. Boake, The design, construction and operation of the LIMPET wave energy converter (Islay, Scotland), in: Proc 4th European

- Wave Energy Conf, Aalborg, Denmark, 2000, pp. 49–55.
- [27] D. Zhang, W. Li, Y. Lin, Wave energy in China: current status and perspectives, *Renew. Energy* 34 (2009) 2089–2092.
- [28] N. Ambli, K. Bonke, O. Malmo, H. Reitan, The Kvaerner multiresonant OWC, in: Proc 2nd Int Symposium Wave Energy Utilization, Trondheim, Norway, 1982, pp. 275–295.
- [29] B. Count, D.V. Evans, The influence of projecting side walls on the hydrodynamic performance of wave energy devices, *J. Fluid Mech.* 145 (1984) 361–376.
- [30] R. Alcorn, S. Hunter, C. Signorelli, R. Obeyesekera, T. Finnigan, T. Denniss, Results of the testing of the Energetech wave energy plant at Port Kembla, *Energetech Rep.* (2005).
- [31] Y. Torre-Enciso, I. Ortubia, L.I. López de Aguilera, J. Marqués, Mutriku wave power plant: from the thinking out to the reality, in: Proc 8th European Wave Tidal Energy Conf, Uppsala, Sweden, 2009, pp. 319–329.
- [32] P. Boccotti, Caisson breakwaters embodying an OWC with a small opening. Part I: theory, *Ocean. Eng.* 34 (2007) 806–819.
- [33] F. Arena, A. Romolo, G. Malara, A. Ascanelli, On design and building of a U-OWC wave energy converter in the Mediterranean sea, in: Proc 32nd Int Conf Ocean Offshore Arct Eng, Nantes, France; 2013, 2013.
- [34] F. Arena, V. Fiamma, V. Laface, G. Malara, et al., Installing U-OWC devices along the Italian coasts, in: Proc 32nd Int Conf Ocean Offshore Arct Eng, Nantes, France, 2013.
- [35] F. Arena, Un impianto REWEC3 per la produzione di energia elettrica da moto ondoso: dall'invenzione del Prof. Paolo Boccotti alla costruzione del primo prototipo, in: Workshop Energia dal Mare le Nuove Tecnologie per i Mari Italiani, Rome, 2014. Available at: http://www.enea.it/it/enea_informa/events/energia-dal-mare/Arena1.pdf (accessed 7.03.15.).
- [36] M.E. McCormick, A theoretical analysis of a self-propelled backward-bent duct wave-energy conversion system, *J. Energy Convers. Technol.-Trans. ASME* 113 (1991) 94–100.
- [37] Y. Masuda, T. Kuboki, M. Ravindran, A.G. Pathak, V. Jayashankar, X.G. Liang, Development of backward bent duct buoy (BBDB), in: Proc 9th Int Offshore Polar Eng Conf, Brest, France, vol. 1, 1999, pp. 142–149.
- [38] Y. Masuda, T. Kuboki, A. Thakker, X.G. Liang, Prospect of economical wave power electric generator by the terminator backward bent duct buoy (BBDB), in: Proc. 12th Int Offshore Polar Eng Conf, Kyushu, Japan, vol. 1, 2002, pp. 607–613.
- [39] D.C. Hong, S.Y. Hong, S.W. Hong, Numerical study of the reverse drift force of floating BBDB wave energy absorbers, *Ocean. Eng.* 31 (2004) 1259–1294.
- [40] K.-R. Lee, W. Koo, M.-H. Kim, Fully nonlinear time-domain simulation of a backward bent duct buoy floating wave energy converter using an acceleration potential method, *Int. J. Nav. Arch. Ocean. Eng.* 5 (2013) 513–528.
- [41] J. Rea, J. Kelly, R. Alcorn, D. O'Sullivan, Development and operation of a power take-off rig for ocean energy research and testing, in: Proc 9th European Wave Tidal Energy Conf, Southampton, 2011.
- [42] R. Alcorn, A. Blavette, M. Healy, A. Lewis, FP7 EU funded CORES wave energy project: a coordinators' perspective on the Galway Bay sea trials, *Underw. Technol.* 32 (2014) 51–59.
- [43] Y. Washio, H. Osawa, Y. Nagata, F. Fujii, H. Furuyama, T. Fujita, The offshore floating type wave power device "Mighty Whale": open sea tests, in: Proc 10th Int Offshore Polar Eng Conf, Seattle, vol. 1, 2000, pp. 373–380.
- [44] T. Ogata, Y. Washio, H. Osawa, Y. Tsuritani, S. Yamashita, Y. Nagata, The open sea tests on the offshore floating type wave power device Mighty Whale: performance of the prototype, in: Proc 21st Int Conf Offshore Mech Arct Eng, Oslo, Norway, 2002. Paper No OMAE2002–28335.
- [45] M.E. McCormick, Analysis of a wave energy conversion buoy, *J. Hydronaut.* 8 (1974) 77–82.
- [46] M.E. McCormick, A modified linear analysis of a wave-energy conversion buoy, *Ocean. Eng.* 3 (1976) 133–144.
- [47] M.E. McCormick, *Ocean Wave Energy Conversion*, Wiley, New York, 1981.
- [48] T.J.T. Whitaker, F.A. McPeake, Design optimization of axisymmetric tail tube buoys, in: D.V. Evans, A.F. de O. Falcão (Eds.), *Hydrodynamics of Ocean Wave Energy Utilization*, Springer, Berlin, 1986, pp. 103–111.
- [49] A. Tucker, J.M. Pemberton, D.T. Swift-Hook, J.M. Swift-Hook, et al., Laminated reinforced concrete technology for the SPEROY wave energy converter, in: Proc XI World Renewable Energy Congress, Abu Dhabi, UAE, 2010, pp. 941–946.
- [50] Nearshore Floating Oscillating Water Column: Prototype Development and Evaluation. Rep. URN 05/581, Department of Trade and Industry, UK, 2005. Available at: <http://webarchive.nationalarchives.gov.uk/2009060903228/http://www.berr.gov.uk/files/file17347.pdf> (accessed 7.03.15.).
- [51] A.F.O. Falcão, J.C.C. Henriques, J.J. Candido, Dynamics and optimization of the OWC spar buoy wave energy converter, *Renew. Energy* 48 (2012) 369–381.
- [52] R.P.F. Gomes, J.C.C. Henriques, L.M.C. Gato, A.F.O. Falcão, Hydrodynamic optimization of an axisymmetric floating oscillating water column for wave energy conversion, *Renew. Energy* 44 (2012) 328–339.
- [53] N. Fonseca, J. Pessoa, S. Ribeiro e Silva, M. Le Boulluec, J. Ohana, Model tests of a wave energy converter based on water oscillating in a U tank, in: 12èmes Journées Hydrodynamique, Nantes France, 2010.
- [54] N. Fonseca, J. Pessoa, Numerical modeling of a wave energy converter based on U-shaped interior oscillating water column, *Appl. Ocean. Res.* 40 (2013) 60–73.
- [55] B.H. Kim, J. Wata, M.A. Zullah, M.R. Ahmed, Y.H. Lee, Numerical and experimental studies on the PTO system of a novel floating wave energy converter, *Renew. Energy* 79 (2015) 111–121.
- [56] D.V. Evans, A submerged cylinder wave energy converter with internal sloshing power take off, *Eur. J. Mech. B-Fluids* 47 (2014) 108–123.
- [57] A. Kurniawan, D. Greaves, J. Chaplin, Wave energy devices with compressible volumes, *Proc. R. Soc. A* 470 (2014) 20140559.
- [58] M. Martinelli, P. Pezzutto, P. Ruol, Experimentally based model to size the geometry of a new OWC device, with reference to the Mediterranean Sea wave environment, *Energies* 6 (2013) 4696–4720.
- [59] J.P. Kofoed, Hydraulic Evaluation of the LEANCON Wave Energy Converter. Dept Civil Engineering, Aalborg University, Denmark, Techn Rep No. 45, 2008. Available at: http://vbn.aau.dk/files/16184099/Hydraulic_Evaluation_of_the_LEACON_Wave_Energy_Converter (accessed 7.03.15.).
- [60] T. Kelly, T. Dooley, J. Campbell, J.V. Ringwood, Comparison of the experimental and numerical results of modelling a 32-oscillating water column (OWC), V-shaped floating wave energy converter, *Energies* 6 (2013) 4045–4077.
- [61] H. Maeda, C.K. Rheem, Y. Washio, H. Osawa, Y. Nagata, T. Ikoma, N. Fujita, M. Arita, Reduction effects of hydroelastic responses on a very large floating structure with wave energy absorption devices using OWC system, in: Proc 20th Int Conf Offshore Mech Arct Eng, Rio de Janeiro, 2001. Paper OMAE2001–5013.
- [62] D.C. Hong, S.Y. Hong, S.W. Hong, Reduction of hydroelastic responses of a very-long floating structure by a floating oscillating-water-column breakwater system, *Ocean. Eng.* 33 (2006) 610–634.
- [63] D.C. Hong, S.Y. Hong, Hydroelastic responses and drift forces of a very-long floating structure equipped with a pin-connected oscillating-water-column breakwater system, *Ocean. Eng.* 34 (2007) 696–708.
- [64] C.M. Wang, Z.Y. Tay, K. Takagi, T. Utsunomiya, Literature review of methods for mitigating hydroelastic response of VLFS under wave action, *Appl. Mech. Rev.* 63 (2010) 030802.
- [65] A.A. Wells, Fluid Driven Rotary Transducer. British patent spec No. 1595700; 1976.
- [66] I.A. Babintsev, Apparatus for Converting Sea Wave Energy into Electrical Energy. U.S. patent No. 3922739; 1975.
- [67] M.E. McCormick, Ocean wave energy concepts, in: Proc Oceans 79 Conf, San Diego (MTS-IEEE), 1979, pp. 553–557.
- [68] S. Raghunathan, The Wells turbine for wave energy conversion, *Prog. Aerosp. Sci.* 31 (1995) 335–386.
- [69] S.L. Dixon, C.A. Hall, *Fluid Mechanics and Thermodynamics of Turbomachinery*, seventh ed., Elsevier, Amsterdam, 2014.
- [70] D.P. Sturge, Turbine for an Oscillating Water Column Wave Power System, CEGB Rep No MM/MECH TA 41, 1977.
- [71] R.J. Grant, C.G. Johnson, D.P. Sturge, Performance of a Wells turbine for use in a wave energy system, in: Future Energy Concepts, IEE, 1981. Publ No 192.
- [72] S. Raghunathan, C.P. Tan, N.A.J. Wells, Theory and performance of a Wells turbine, *J. Energy* 6 (1982) 157–160.
- [73] T. von Kármán, J.M. Burgers, General aerodynamic theory – perfect fluids, in: W.F. Durand (Ed.), *Aerodynamic Theory*, vol. 2, Springer, Berlin, 1934.
- [74] F.S. Weinig, Theory of two-dimensional flow through cascades, in: W.R. Hawthorne (Ed.), *Aerodynamics of Turbines and Compressors*, Oxford University Press, London, 1964, pp. 13–82.
- [75] N. Scholz, *Aerodynamics of Cascades*. AGARD-AG-220, 1977.
- [76] L.M.C. Gato, A.F. de O. Falcão, Performance of the Wells turbine with double row of guide vanes, *JSME Int. J.-Ser. II* 33 (1990) 265–271.
- [77] S. Raghunathan, C.P. Tan, The performance of the biplane Wells turbine, *J. Energy* 7 (1983) 741–742.
- [78] R. Arlett, H.-U. Banzhaf, R. Starzmann, F. Biskup, Air Turbine for Wave Power Station. Patent No. WO 2009/089902; 2009.
- [79] A.F.O. Falcão, J.C.C. Henriques, L.M.C. Gato, R.P.F. Gomes, Air turbine choice and optimization for floating oscillating-water-column wave energy converter, *Ocean. Eng.* 75 (2014) 148–156.
- [80] T. Setoguchi, T.H. Kim, K. Kaneko, M. Takao, Y.W. Lee, M. Inoue, Air turbine with staggered blades for wave power conversion, in: Proc 12th Int Offshore Polar Eng Conf, 2002, pp. 662–667.
- [81] T. Setoguchi, S. Sathakumar, M. Takao, T.H. Kim, K. Kaneko, A modified Wells turbine for wave energy conversion, *Renew. Energy* 28 (2003) 79–91.
- [82] J.R.M. Taylor, N.J. Caldwell, Design and construction of the variable-pitch air turbine for the Azores wave energy plant, in: Proc 3rd European Wave Energy Conf, Patras, Greece, 1998, pp. 328–337.
- [83] D. Richards, F.B. Weiskopf, Studies with and testing of the McCormick pneumatic wave energy turbine with some comments on PWECS systems, in: M.E. McCormick, Y.C. Kim (Eds.), *Utilization of Ocean Waves – Wave to Energy Conversion*, ASCE, New York, 1986, pp. 80–102.
- [84] T.W. Kim, K. Kaneko, T. Setoguchi, M. Inoue, Aerodynamic performance of an impulse turbine with self-pitch-controlled guide vanes for wave power generator, in: Proc 1st KSME-JSME Thermal Fluid Eng Conf, vol. 2, 1988, pp. 133–137.
- [85] C. Freeman, S.J. Herring, K. Banks, Impulse Turbine for Use in Bi-directional Flows. Patent No. WO 2008/012530 A2; 2008.
- [86] S. Natanzai, J.A. Teixeira, G. Laird, A novel high-efficiency impulse turbine for use in oscillating water column devices, in: Proc 9th European Wave Tidal Energy Conf, Southampton, UK, 2011.
- [87] R. Curran, T. Denniss, C. Boake, Multidisciplinary design for performance: ocean wave energy conversion, in: Proc 10th Int Offshore Polar Eng Conf, Seattle, vol. 1, 2000, pp. 434–441.

- [88] T. Finnigan, D. Auld, Model testing of a variable-pitch aerodynamic turbine, in: Proc 13th Int Offshore Polar Eng Conf, Honolulu, 2003, pp. 357–360.
- [89] M.E. McCormick, J.G. Rehak, B.D. Williams, An experimental study of a bi-directional radial turbine for pneumatic conversion, in: Proc Mastering Ocean through Technol, vol. 2, 1992, pp. 866–870.
- [90] M.E. McCormick, B. Cochran, A performance study of a bi-directional radial turbine, in: Proc European Wave Energy Symp, Edinburgh, 1993, pp. 443–448.
- [91] M. Takao, K. Itakura, T. Setoguchi, T.H. Kim, K. Kaneko, A. Thakker, Performance of a radial turbine for wave power conversion, in: Proc 12th Int Offshore Polar Eng Conf, Kitakyushu, Japan, 2002, pp. 562–567.
- [92] F. Castro, A. el Marjani, M.A. Rodriguez, T. Parra, Viscous flow analysis in a radial impulse turbine for OWC wave energy systems, in: Proc 7th European Wave Tidal Energy Conf, Porto, Portugal, 2007.
- [93] B. Pereiras, F. Castro, A. el Marjani, M.A. Rodriguez, Radial impulse turbine for wave energy conversion. A new geometry, in: Proc 27th Int Conf Offshore Mech Arct Eng, Estoril, Portugal, 2008. Paper OMAE2008–57951.
- [94] B. Pereiras, F. Castro, A.A. Rodriguez, Tip clearance effect on the flow pattern of a radial impulse turbine for wave energy conversion, in: Proc 9th Int Offshore Polar Eng Conf, Osaka, 2009, pp. 290–298.
- [95] B. Pereiras, F. Castro, A. el Marjani, M.A. Rodriguez, An improved radial impulse turbine for OWC Renew. Energy 36 (2011) 1477–1484.
- [96] M. Takao, Y. Fujioka, T. Setoguchi, Effect of pitch-controlled guide vanes on the performance of a radial turbine for wave energy conversion, Ocean. Eng. 32 (2005) 2079–2087.
- [97] J.A.C. Kentfield, A bidirectional flow air-turbine for wave energy extraction, in: Proc 6th. Int Conf Alternative Energy Sources, Miami Beach, 1983, pp. 59–60.
- [98] C. Moisel, R. Starzmann, Aerodynamic design and numerical investigation of a new radial bi-directional turbine for wave energy conversion, in: Proc 10th European Wave Tidal Energy Conf, Aalborg, Denmark, 2013.
- [99] C. Moisel, T.H. Carolus, Experimental loss analysis on a model-scale radial bidirectional air-turbine for wave energy conversion, in: Proc 1st International Conf Renew Energies Offshore, Lisbon, 2014.
- [100] Y. Osada, T. Konno, Air Turbine for Wave Power Generation. Japanese patent JP2008095569(A); 2008.
- [101] T. Konno, Y. Nagata, M. Takao, T. Setoguchi, Experimental study of a radial turbine using floating nozzle for wave energy conversion. In: Proc 29th Int Conf Ocean Offshore Arct Eng, Honolulu, Hawaii; 2009, Paper OMAE2009–80076.
- [102] L.M.C. Gato, A.F.O. Falcão, Turbine with Radial Inlet and Outlet Flow Rotor for Use in Bi-directional Flows. Patent WO2011012746 A4; 2012.
- [103] A.F.O. Falcão, L.M.C. Gato, E.P.A.S. Nunes, A novel radial self-rectifying air turbine for use in wave energy converters, Renew. Energy 50 (2013) 289–298.
- [104] A.F.O. Falcão, L.M.C. Gato, E.P.A.S. Nunes, A novel radial self-rectifying air turbine for use in wave energy converters. Part 2. Results from model testing, Renew. Energy 53 (2013) 159–164.
- [105] V. Jayashankar, S. Anand, T. Geetha, S. Santhakumar, V.J. Kumar, M. Ravindran, T. Setoguchi, M. Takao, K. Toyota, S. Nagata, A twin unidirectional impulse turbine topology for OWC based wave energy plants, Renew. Energy 34 (2009) 692–698.
- [106] K. Mala, J. Jayara, V. Jayashankar, T.M. Muruganandam, S. Santhakumar, M. Ravindran, M. Takao, T. Setoguchi, K. Toyota, S. Nagata, A twin unidirectional impulse turbine topology for OWC based wave energy plants – experimental validation and scaling, Renew. Energy 36 (2011) 307–314.
- [107] V. Jayashankar, K. Mala, J. Jayaraj, T. Setoguchi, M. Takao, A twin unidirectional turbine topology for wave energy, in: Proc 3rd Int Conf Ocean Energy, Bilbao, Spain, 2010.
- [108] B. Pereiras, P. Valdez, F. Castro, Numerical analysis of a unidirectional axial turbine for twin turbine configuration, Appl. Ocean. Res. 47 (2014) 1–8.
- [109] M. Suzuki, C. Arakawa, S. Takahashi, Performance of wave power generating system installed in breakwater at Sakata port in Japan, in: Proc 14th Int Offshore Polar Eng Conf, Toulon, France, 2004, pp. 202–209.
- [110] V.S. Raju, M. Ravindran, P.M. Koola, Experiences on a 150 kW wave energy pilot plant, in: Proc European Wave Energy Symp, Edinburgh, 1993, pp. 277–282.
- [111] S. Raghunathan, R. Curran, T.J.T. Whittaker, Performance of the Islay Wells air turbine, Proc. Inst. Mech. Eng. Part A: J. Power Energy 209 (1995) 55–62.
- [112] N.J. Caldwell, J.R.M. Taylor, Eddy-current actuator for a variable pitch air turbine, in: Proc 3rd European Wave Energy Conf, Patras, Greece, 1998, pp. 104–110.
- [113] T.V. Heath, The development of a turbo-generation system for application in OWC breakwaters, in: Proc 7th European Wave Tidal Energy Conf, Porto, Portugal, 2007.
- [114] Islay LIMPET Wave Power Plant, Publishable Report. Contract JOR-CT98-0312, The European Commission, 2002.
- [115] T.J.T. Whittaker, W. Beattie, M. Folley, C. Boake, A. Wright, M. Osterried, T. Heath, Performance of the LIMPET wave power plant – Prediction, measurement and potential, in: Proc 5th European Wave Energy Conf, Cork, Ireland, 2003, pp. 97–104.
- [116] M. Takao, T. Setoguchi, K. Kaneko, S. Raghunathan, M. Inoue, Noise characteristics of turbines for wave power conversion, Proc. Inst. Mech. Eng. Part A: J. Power Energy 216 (2002) 223–228.
- [117] R. Starzmann, T. Carolus, Model-based selection of full-scale Wells turbines for ocean wave energy conversion and prediction of their aerodynamic and acoustic performances, Proc. Inst. Mech. Eng. Part A: J. Power Energy 228 (2014) 2–16.
- [118] A.F.O. Falcão, J.C.C. Henriques, Model-prototype similarity of oscillating-water-column wave energy converters, Int. J. Mar. Energy 6 (2014) 18–34.
- [119] A.F. de O. Falcão, R.J.A. Rodrigues, Stochastic modelling of OWC wave power plant performance, Appl. Ocean. Res. 24 (2002) 59–71.
- [120] Y. Kamizuru, C. Fissmann, H. Murrenhoff, Hydrostatic drive trains for wave energy converters: simulation and experiments for efficient design, in: Proc 10th European Wave Tidal Energy Conf, Aalborg, 2013.
- [121] A.F. de O. Falcão, Stochastic modelling in wave power-equipment optimization: maximum energy production versus maximum profit, Ocean. Eng. 31 (2004) 1407–1421.
- [122] A.F. de O. Falcão, A.J.N.A. Sarmento, Wave generation by a periodic surface-pressure and its application in wave-energy extraction, in: 15th Int Congr Theor Appl Mech, Toronto, 1980.
- [123] D.V. Evans, Wave-power absorption by systems of oscillating surface pressure distributions, J. Fluid Mech. 114 (1982) 481–499.
- [124] J.V. Wehausen, E.V. Laitone, Surface waves, in: Encyclopedia of Physics, Vol. IX Fluid Dynamics III, Springer Verlag, Berlin, 1960, pp. 446–778.
- [125] J.V. Wehausen, The motion of floating bodies, Annu. Rev. Fluid Mech. 3 (1971) 237–268.
- [126] D.V. Evans, Theory for wave-power absorption by oscillating bodies, J. Fluid Mech. 77 (1976) 1–25.
- [127] J. Falnes, Ocean Waves and Oscillating Systems, Cambridge University Press, Cambridge, 2002.
- [128] W.E. Cummins, The impulse response function and ship motions, Schiffstechnik 9 (1962) 101–109.
- [129] E.R. Jefferys, Device characterisation, in: B. Count (Ed.), Power from Sea Waves, Academic Press, London, 1980, pp. 413–438.
- [130] A.F. de O. Falcão, P.A.P. Justino, OWC wave energy conversion with valve-constrained flow, in: Proc 2nd European Wave Power Conf, Lisbon, 1995, pp. 187–194.
- [131] J. Falnes, P. McIver, Surface wave interactions with systems of oscillating bodies and pressure distributions, Appl. Ocean. Res. 7 (1985) 225–234.
- [132] D.V. Evans, R. Porter, Hydrodynamic characteristics of an oscillating water column device, Appl. Ocean. Res. 17 (1995) 155–164.
- [133] D.V. Evans, R. Porter, Efficient calculation of hydrodynamic properties of OWC-type devices, J. Offshore Mech. Arct. Eng.-Trans. ASME 119 (1997) 210–218.
- [134] H. Martin-Rivas, C.C. Mei, Wave power extraction from an oscillating water column at the tip of a breakwater, J. Fluid Mech. 626 (2008) 395–414.
- [135] S. Lovas, C.C. Mei, Y. Liu, Oscillating water column at a coastal corner for wave power extraction, Appl. Ocean. Res. 32 (2010) 267–283.
- [136] S.A. Mavrakos, D.N. Konispoliatis, Hydrodynamics of a free floating vertical axisymmetric oscillating water column device, J. Appl. Math. 2012 (2012). Article No. 14280.
- [137] K. Rezanejad, J. Bhattacharjee, C.G. Soares, Analytical and numerical study of dual-chamber oscillating water columns on stepped bottom, Renew. Energy 75 (2015) 272–282.
- [138] A.F. de O. Falcão, Wave-power absorption by a periodic linear array of oscillating water columns, Ocean. Eng. 29 (2002) 1163–1186.
- [139] G.C. Nihous, Wave power extraction by arbitrary arrays of non-diffracting oscillating water columns, Ocean. Eng. 51 (2012) 94–105.
- [140] A. Brito-Melo, A.J.N.A. Sarmento, A.H. Clément, G.A. Delhommeau, 3D boundary element code for the analysis of OWC wave-power plants, in: Proc 9th Int Offshore Polar Eng Conf, Brest France, vol. 1, 1999, pp. 188–195.
- [141] A. Brito-Melo, T. Hofmann, A.J.N.A. Sarmento, A.H. Clément, G. Delhommeau, Numerical modelling of OWC-shoreline devices including the effect of surrounding coastline and non-flat bottom, Int. J. Offshore Polar Eng. 11 (2001) 147–154.
- [142] C.H. Lee, J.N. Newman, F.G. Nielsen, Wave interactions with an oscillating water column, in: Proc 6th Int Offshore Polar Eng Conf, Los Angeles, 1996.
- [143] Y. Zhang, Q.P. Zhou, D. Greaves, Air-water two-phase flow modelling of hydrodynamic performance of an oscillating water column device, Renew. Energy 41 (2012) 159–170.
- [144] Y.Y. Luo, J.R. Nader, P. Cooper, S.P. Zhu, Nonlinear 2D analysis of the efficiency of fixed oscillating water column wave energy converters, Renew. Energy 64 (2013) 255–265.
- [145] P.R.F. Teixeira, D.P. Davyt, E. Didier, R. Ramalhais, Numerical simulation of an oscillating water column device using a code based on Navier-Stokes equations, Energy 61 (2013) 513–530.
- [146] I. Lopez, B. Pereiras, F. Castro, G. Iglesias, Optimization of turbine-induced damping for an OWC wave energy converter using a RANS–VOF numerical model, Appl. Energy 127 (2014) 105–114.
- [147] Y. Luo, Z. Wang, G. Peng, Y. Xiao, L. Zhai, X. Liu, Q. Zhang, Numerical simulation of a heave-only floating OWC (oscillating water column) device, Energy 76 (2014) 799–806.
- [148] A. Karmath, H. Bihs, O.A. Arntsen, Numerical modeling of power take-off damping in an oscillating water column device, Int. J. Mar. Energy 10 (2015) 1–16.
- [149] A.J.N.A. Sarmento, A.F. de O. Falcão, Wave generation by an oscillating surface-pressure and its application in wave-energy extraction, J. Fluid Mech. 150 (1985) 467–485.
- [150] R. Jefferys, T. Whittaker, Latching control of an oscillating water column device with air compressibility, in: D.V. Evans, A.F. de O. Falcão (Eds.),

- Hydrodynamics of Ocean Wave Energy Utilization, Springer, Berlin, 1986, pp. 281–291.
- [151] W. Sheng, R. Alcorn, A. Lewis, On thermodynamics in the primary power conversion of oscillating water column wave energy converters, *J. Renew. Sust. Energy* 5 (2013) 023105.
- [152] A.F. de O. Falcão, P.A.P. Justino, OWC wave energy devices with air-flow control, *Ocean. Eng.* 26 (1999) 1275–1295.
- [153] G. Payne, Guidance for the Experimental Tank Testing of Wave Energy Converters. SuperGen Marine Rep., Univ. Edinburgh, 2008. Available at: http://www.supergen-marine.org.uk/drupal/files/reports/WEC_tank_testing.pdf (accessed 7.03.15).
- [154] V. Heller, Development of wave devices from initial conception to commercial demonstration, in: A. Sayigh (Ed.), Comprehensive Renewable Energy vol. 8, Ocean Energy, Elsevier, Oxford, 2012, pp. 79–110.
- [155] W. Sheng, R. Alcorn, T. Lewis, Physical modelling of wave energy converters, *Ocean. Eng.* 84 (2014) 29–36.
- [156] J. Weber, Representation of non-linear aero-thermodynamic effects during small scale physical modelling of OWC WECs, in: Proc 7th European Wave Tidal Energy Conf, Porto, Portugal, 2007.
- [157] L.H. Holthuijsen, Waves in Oceanic and Coastal Waters, Cambridge University Press, Cambridge, 2007.
- [158] A.J.N.A. Sarmento, Model tests optimisation of an OWC wave power plant, *Int. J. Offshore Polar Eng.* 3 (1993) 66–72.
- [159] S.H. Salter, D.C. Jeffery, J.R.M. Taylor, The architecture of nodding duck wave power generators, *Nav. Arch.* 1 (1976) 21–24.
- [160] J. Falnes, K. Budal, Wave power conversion by point absorbers, *Nor. Marit. Res.* 6 (1978) 2–11.
- [161] J. Falnes, Optimum control of oscillation of wave-energy converters, *Int. J. Offshore Polar Eng.* 12 (2002) 147–155.
- [162] L.M.C. Gato, A.F.O. de Falcão, Aerodynamics of the Wells turbine: control by swinging rotor blades, *Int. J. Mech. Sci.* 31 (1989) 425–434.
- [163] A.J.N.A. Sarmento, L.M.C. Gato, A.F. de O. Falcão, Turbine-controlled wave energy absorption by oscillating water column device, *Ocean. Eng.* 17 (1990) 481–497.
- [164] L.M.C. Gato, L.R.C. Eça, A.F. de O. Falcão, Performance of the Wells turbine with variable pitch rotor blades, *J. Energ. Resour. Technol.-Trans. ASME* 113 (1991) 141–146.
- [165] J. Perdigão, A. Sarmento, Overall-efficiency optimisation in OWC devices, *Appl. Ocean. Res.* 25 (2003) 157–166.
- [166] R.E. Hoskin, B.M. Count, N.K. Nichols, D.A.C. Nicol, Phase control for the oscillating water column, in: D.V. Evans, A.F. de O. Falcão (Eds.), Hydrodynamics of Wave-energy Utilization, Springer, Berlin, 1986, pp. 257–268.
- [167] N.J. Caldwell, J.R.M. Taylor, Design and construction of elastomeric parts for the Azores OWC high speed valve, in: Proc 3rd European Wave Energy Conf, Patras, Greece, 1998, pp. 318–327.
- [168] J.C.C. Henriques, J.C. Chong, A.F.O. Falcão, R.P.F. Gomes, Latching control of a floating oscillating water column wave energy converter in irregular waves, in: Proc 33rd Int Conf Ocean Offshore Arct Eng, San Francisco, 2014. Paper OMAE 2014–23260.
- [169] M.F.P. Lopes, J. Hals, R.P.F. Gomes, T. Moan, L.M.C. Gato, A.F. de O. Falcão, Experimental and numerical investigation of non-predictive phase-control strategies for a point-absorbing wave energy converter, *Ocean. Eng.* 36 (2009) 386–402.
- [170] J.C.C. Henriques, A.F.O. Falcão, R.P.F. Gomes, L.M.C. Gato, Latching control of an oscillating water column spar-buoy wave energy converter in regular waves, *J. Offshore Mech. Arct. Eng. Trans. ASME* 135 (2013) 021902.
- [171] J.C.C. Henriques, J.C. Chong, A.F.O. Falcão, R.P.F. Gomes, Latching control of a floating oscillating water column wave energy converter in irregular waves, in: Proc 33rd Int Conf Ocean Offshore Arct Eng, San Francisco, 2014. Paper No. OMAE 2014–23260.
- [172] A.F. de O. Falcão, Control of an oscillating water column wave power plant for maximum energy production, *Appl. Ocean. Res.* 24 (2002) 73–82.
- [173] M. Amundarain, M. Alberdi, A.J. Garrido, I. Garrido, Neural rotational speed control for wave energy converters, *Int. J. Control.* 84 (2011) 293–309.
- [174] A.F. de O. Falcão, L.C. Vieira, P.A.P. Justino, J.M.C.S. André, By-pass air-valve control of an OWC wave power plant, *J. Offshore Mech. Arct. Eng. Trans. ASME* 125 (2003) 205–210.
- [175] K. Monk, D. Conley, M. Lopes, Q. Zou, Pneumatic power regulation by wave forecasting and real-time relief valve control for an OWC, in: Proc 10th European Wave Tidal Energy Conf, Aalborg, Denmark, 2013.